

THIS IS A PREPRINT --- SUBJECT TO CORRECTION

The Isochronal Testing of Oil Wells

By

M. J. Fetkovich, Member AIME, Phillips Petroleum Co.

© Copyright 1973
American Institute of Mining, Metallurgical, and Petroleum Engineers, Inc.

This paper was prepared for the 48th Annual Fall Meeting of the Society of Petroleum Engineers of AIME, to be held in Las Vegas, Nev., Sept. 30-Oct. 3, 1973. Permission to copy is restricted to an abstract of not more than 300 words. Illustrations may not be copied. The abstract should contain conspicuous acknowledgment of where and by whom the paper is presented. Publication elsewhere after publication in the JOURNAL OF PETROLEUM TECHNOLOGY or the SOCIETY OF PETROLEUM ENGINEERS JOURNAL is usually granted upon request to the Editor of the appropriate journal provided agreement to give proper credit is made.

Discussion of this paper is invited. Three copies of any discussion should be sent to the Society of Petroleum Engineers office. Such discussion may be presented at the above meeting and, with the paper, may be considered for publication in one of the two SPE magazines.

ABSTRACT

This paper presents the results and methods of analyzing isochronal and flow after flow multipoint back-pressure tests conducted on oil wells. Tests were conducted in reservoirs with permeabilities ranging from 6 MD to > 1000 MD. Reservoirs in which oil well multipoint back-pressure tests were obtained ranged from highly undersaturated, to saturated at initial reservoir pressure, to a partially depleted field with a gas saturation existing above the critical. Each of these three reservoir fluid states can result in different interpretation methods. Back-pressure tests were run to pseudo-steady state in the field where the saturation was above the critical gas saturation.

In all cases, oil well back-pressure curves were found to follow the same general form as that used to express the rate-pressure relationship of a gas well:

$$q_o = J_o' (\bar{p}_R^2 - p_{wf}^2)^n$$

From some 40 oil well back-pressure tests examined, the exponent n was found to lie between 0.568 and 1.000, very near the limits commonly accepted for gas well back-pressure

References and illustrations at end of paper.

curves. Flow point alignment to establish an oil well back-pressure curve on the customary $\log q_o$ vs. $\log \Delta(p^2)$ plot is considered to be as good as that obtained on gas well back-pressure tests.

This paper demonstrates that gas wells and oil wells behave very similarly and should be tested and analyzed using the same basic flow equations.

INTRODUCTION

Multipoint back-pressure testing of gas wells is an accepted procedure for establishing a gas well's performance curve. Flow after flow¹ and isochronal² testing are the two basic methods commonly used. In high permeability reservoirs, either method can be employed. In low permeability reservoirs, the Isochronal method of testing eliminates the transient effects that can severely distort the results obtained from a flow after flow test. Methods for analyzing and calculating gas well performance curves have been the subject of numerous investigations. The bulk of these investigations have examined non-Darcy flow behavior, the primary reason that multipoint tests are conducted.

Multipoint testing of oil wells is not now a current practice. As early as 1930, however,

T. V. Moore³ reported the results of an oil well multipoint test conducted on the Humble Smith A-2 in the Yates Field. The purpose of the back-pressure test was to demonstrate a method of establishing a well's open flow potential without producing the well wide open.

The need for establishing an accurate performance curve for an oil well is as important as determining one for a gas well. In the search for new oil, the industry is turning to remote areas such as the Arctic and offshore. Critical questions of whether to develop, and if so, how to develop a field hinge on the ability to accurately predict a well's deliverability. Often, because of equipment limitations, the rates of production obtained during drillstem testing are much less than those planned for full development.

The traditional method for predicting production rates and drawdowns for oil wells has been based on the concept of the productivity index (PI), which has been used in the oil industry for many years. The usual form of the equation

$$q_o = J_o (p_e - p_{wf}) \dots \dots \dots (1)$$

is valid only for systems producing an ideal homogeneous liquid obeying Darcy's law. This condition normally holds for oil wells when the oil is undersaturated throughout the producing formation. It has long been recognized that in reservoirs existing at or below the bubble-point pressure, producing wells do not follow this simple equation. Actual field tests indicate that oil flow rates obtained at increasing drawdowns decline much faster than would be predicted by Eq. 1.

Evinger and Muskat⁴ first derived a theoretical productivity index for steady state radial flow in an attempt to account for the observed non-linear flow behavior of oil wells and arrived at the following equation

$$q_o = \frac{7.08 kh}{\ln \left(\frac{r_e}{r_w} \right)} \int_{p_{wf}}^{p_e} f(p) dp \dots \dots (2)$$

$$\text{where } f(p) = \frac{k_{ro}}{u_o B_o}$$

Calculations using Eq. 2 based on typical reservoir and fluid properties indicated that PI at a fixed reservoir pressure p_e (as defined from Eq. 1) decreases with increasing drawdown.

In a computer study by Vogel⁵, results based on two-phase flow theory were presented to indicate that a single empirical inflow performance relationship (IPR) equation might

be valid for most solution-gas drive reservoirs. He found that a single dimensionless IPR equation approximately held for several hypothetical solution-gas drive reservoirs even when using a wide range of oil PVT properties and reservoir relative permeability curves. The fact that his study covered a wide range of fluid properties and relative permeability curves to obtain a single reference curve, can not be over emphasized. Vogel then proposed that his equation be used to take the place of the linear productivity index relationship for solution-gas drive reservoirs when the reservoir pressure is at or below the bubble-point pressure.

The proposed empirical reference equation (IPR) in dimensionless form was given as

$$\frac{q_o}{(q_o)_{\max}} = 1 - 0.20 \left(\frac{p_{wf}}{\bar{p}_R} \right) - 0.80 \left(\frac{p_{wf}}{\bar{p}_R} \right)^2 \dots (3)$$

A comparison was made of IPR's for liquid flow, gas flow ($n=1$) and two-phase flow (his reference curve) on a dimensionless basis, (Fig. 1). As is evident from Fig. 1 the position of the two-phase reference curve relative to liquid and gas flow indicates that oil wells producing as if in a solution-gas drive reservoir should actually behave more like a gas well, i.e., $(\bar{p}_R^2 - p_{wf}^2)$ vs. q_o should plot as a straight line on log-log paper with a slope (n) near unity.

This paper presents the results of multipoint back-pressure tests taken at a single reservoir pressure level (\bar{p}_R). These results show that the performance curve for an oil well can be expressed by a more general and familiar equation similar to that used for gas wells,

$$q_o = J_o' (\bar{p}_R^2 - p_{wf}^2)^n \dots \dots \dots (4)$$

Reservoirs in which oil well multipoint back-pressure tests were obtained ranged from highly undersaturated, to saturated at initial reservoir pressure, to a partially depleted field with a gas saturation existing above the critical (equilibrium) gas saturation. Equation 4 was found to be valid for tests conducted in all three reservoir fluid states, even for the conditions where flowing pressures were well above the bubble-point pressure. Permeabilities of the reservoirs ranged from 6 to >1000 millidarcys. Flow point alignment to establish an oil well back-pressure curve on the customary $\log q_o$ vs. $\log \Delta(p^2)$ was found to be as good as that obtained on gas well back-pressure tests.

BASIC EQUATIONS AND PRESSURE FUNCTIONS

The basic flow equation given by Evinger and Muskat⁴ for steady-state flow, applicable to either oil or gas flow, is

$$q_o = \frac{7.08 kh}{\ln\left(\frac{r_e}{r_w}\right)} \int_{P_{wf}}^{P_e} f(p) dp \dots (2)$$

where $f(p)$ can be any function of pressure. Using the typical pressure function depicted in Fig. 2 it is obvious that we can evaluate the total integral in two parts and write

$$q_o = \left[\frac{7.08 kh}{\ln\left(\frac{r_e}{r_w}\right) + s'} \int_{P_{wf}}^{P_b} \frac{k_{ro}(S,p)}{u_o B_o} dp + \int_{P_b}^{P_e} \frac{k_{ro}(p)}{u_o B_o} dp \right] \dots (5)$$

For flow in the region where the pressures are above the bubble point pressure if we assume $k_{ro} = 1$ (neglecting the pressure dependent permeability term for simplicity of presentation only) and treat $(u_o B_o)$ evaluated at the average pressure $(p_e + p_b)/2$ we can write

$$q_o = \left[\frac{7.08 kh}{\ln\left(\frac{r_e}{r_w}\right) + s'} \int_{P_{wf}}^{P_b} \frac{k_{ro}(S,p)}{u_o B_o} dp + \frac{(p_e - P_b)}{(u_o B_o)} \right] \dots (6)$$

Except for the addition of the necessary skin term, s' (discussed later in the paper) Eq. 6 is identical to that derived by Handy²¹.

Figure 2 illustrates a plot of $1/u_o B_o$ as a function of pressure for an undersaturated oil reservoir. Also, drawn on this figure is a dashed line representing the effect of relative permeability (k_{ro}) on drawdowns below the bubble-point pressure. It is assumed for purposes of demonstration that $k_{ro}/(u_o B_o)$ is linear and its intercept is 0 at P_o pressure. The simplifying assumption of the 0 intercept for $k_{ro}/(u_o B_o)$ approximately defines Vogel's IPR curve and exactly defines Eq. 4 when $n=1$. Also, drawn on Fig. 2 is a hypothetical pressure function $k_{ro}/(u_o B_o)$ represented as a constant for all pressures. It is clear that a constant value of $k_{ro}/(u_o B_o)$ over the entire pressure drawdown range is required to obtain a constant productivity index (PI).

Figure 3 illustrates plots of $1/(u_o B_o)$ for two high pressure gas reservoirs. Curve E_A was obtained from calculations using the reservoir gas analysis and standard correlations of Z and u_g as functions of critical pressure and temperature. Curve B was obtained directly from a PVT study. One striking feature of curve A is the fact that it resembles that of an under-

saturated oil reservoir with an apparent or pseudo bubble-point pressure near 2500 psia, the normal inflection point of a Z curve. A further observation that can be made from curves A and B is that a region exists where a gas well can be considered to behave as a liquid, i.e., $1/(u_o B_o)$ is nearly constant or only slightly changing with pressure as is the case for the pressure function of an undersaturated oil reservoir above the bubble-point pressure.

For the region where the pressure function is a constant, or nearly so, we can immediately write upon integration of Eq. 2 the well known steady-state single phase flow equation:

$$q = \frac{7.08 kh}{\ln\left(\frac{r_e}{r_w}\right) + s'} \frac{(P_e - P_{wf})}{(u_o B_o)} \dots (7)$$

Note that this equation would approximately hold for gas wells represented by curves A and B in Fig. 3 over a considerable range of pressure drawdowns. q_g will then be proportional to Δp instead of $\Delta(p^2)$. This, in fact was found to be the case for isochronal tests conducted on two wells in a reservoir with fluid properties represented by curve B.

Now considering the entire pressure function from p_e to 0, for either the oil or gas curves, (the dashed line in Fig. 2) we note that $f(p)$ can be represented approximately by two separate straight line segments. The approximate flow equation then, over the total pressure interval, can be written as: (See Appendix)

$$q = \frac{7.08 kh}{\left[\ln\left(\frac{r_e}{r_w}\right) + s' \right] (u_o B_o)_{P_e, P_b}} \left[\frac{(u_o B_o)_{P_e, P_b} a_2}{2} (P_b^2 - P_{wf}^2) + (P_e - P_b) \right] \dots (8)$$

or $q = J' (P_b^2 - P_{wf}^2) + J (P_e - P_b) \dots (8A)$

For drawdowns both above and below the bubble-point pressure, a back-pressure curve plot will appear as two line segments, with the intersection yielding an approximate value for the reservoir bubble-point pressure. This then offers an approach for determining a reservoir's bubble-point pressure from an isochronal test. For an isochronal test, a constant reservoir radius of investigation is obtained for each flow—an insitu constant volume cell.

If the degree of undersaturation is slight, the two line segments may not be definable. Unstable flow conditions in the tubing at the

low flow rates necessary to define the single-phase flow conditions may preclude defining two straight lines. Further, as will be demonstrated later, non-Darcy flow can exist even when all flowing pressures are above the bubble-point pressure. Conceivably then this could lead to even three line segments.

For the case of all drawdowns below the bubble-point pressure $J(p_e - p_b)$ is a constant, while the remaining term varies non-linearly with flowing pressure, p_{wf} .

The composite effect results in an equation of the form

$$q = C (p_e^2 - p_{wf}^2)^n \dots \dots \dots (9)$$

As p_e decreases to the pressure p_b , $n \rightarrow 1.0$ and $C \rightarrow J'$ such that for the oil well case, only the two-phase flow term remains. We thus obtain the basic equation suggested from Vogel's results for $p_e \leq p_b$:

$$q_o = J'_o (p_e^2 - p_{wf}^2)^{1.0} \dots \dots \dots (10)$$

A significant conclusion to be drawn from Eq. 9 is that a gas well or an oil well can have a slope less than 1.0 on a $\log q$ vs. $\log \Delta(p^2)$ plot without non-Darcy flow existing. The slope (n) in this case is strictly a result of the shape of the wells pressure function. This possibility, for a gas well, was recognized and reported by Rowan and Clegg⁶.

Eq. 10 must be further generalized with an exponent (n) in light of results obtained from multipoint back-pressure tests conducted on oil wells for both single-phase and two-phase flow to

$$q_o = J'_o (p_e^2 - p_{wf}^2)^n \dots \dots \dots (11)$$

Eq. 11 is identical in form to the gas well back-pressure equation. For constant rate transient gas flow, the gas well back-pressure equation is usually expressed by^{7,8}

$$\frac{7.08 kh (p_i - p_{wf})}{q(uB)} = \ln \sqrt{\frac{14.23 k_i t}{\phi (uc_t)_i r_w^2}} + s + Dq \dots \dots (12)$$

Other than for the unique fluid property cases discussed above, or a pressure dependent permeability effect, the non-Darcy flow term in Eq. 12 is required to obtain an exponent (n) less than 1.0.

In terms of a pseudo-pressure⁹ $m(p)$

$$\frac{7.08 kh [m(p_i) - m(p_{wf})]}{q} =$$

$$\ln \sqrt{\frac{14.23 k_i t}{\phi (uc_t)_i r_w^2}} + s + Dq \dots \dots (13)$$

where $m(p)$ can also include a pressure dependent permeability^{10,11}

$$m(p) = \int_0^p \frac{k_{ro}(S,p)}{uB} dp \dots \dots (14)$$

(The effect of a pressure dependent permeability could readily be displayed in Figs. 2 and 3.)

Equation 12 or 13 then should be applicable for analyzing both oil well and gas well back-pressure tests.

RATE AND TIME DEPENDENT SKIN, $s(q,t)$

Slopes much less than 1 were consistently obtained from isochronal tests conducted on oil wells in saturated reservoirs. For undersaturated reservoirs, the shape of the pressure function was shown to be capable of accounting for slopes less than 1. Since Vogel's work based on two-phase flow theory indicated back-pressure curve slopes should be unity or even greater, a near well bore effect was suspected. (All of Vogel's results show the first calculated IPR curve after 0.1% of original oil-in-place is recovered. The effect of initial gas saturation build-up around the wellbore may not have been present in his results.) Handy²¹ studied the adverse effect on PI of two-phase flow in the vicinity of the wellbore for undersaturated oils. Muskat^{12,13} presented a simple approach to study the effect of two-phase flow about the well bore for a gas condensate well that could be applied to a saturated or undersaturated gas condensate or oil well.

$s(q,t)$ FOR CONDENSATE WELLS

Muskat's equation to calculate the rate of change of liquid saturation taking place about the wellbore for a producing condensate well is:

$$\frac{dS}{dt} = \frac{q_g}{2\pi rh\phi} \frac{dp}{dr} \frac{dc}{dp} \dots \dots (15)$$

Saturation is assumed to build up only to the limiting equilibrium liquid saturation; its radius then expanding with time. For a steady state pressure distribution, and saturation S equal to 0 at $t=0$, we can obtain an equation

in terms of the approximate radius of the equilibrium two-phase flow region. In engineering units it is

$$r_a^2 = \frac{.1135 q_g^2 uZYt}{h^2 \phi k \bar{p} S_{clh}} \dots (16)$$

where Y is expressed as reservoir cubic feet of condensate accumulation in the reservoir per Mscf of full wellstream gas produced per psi, $\frac{dc}{dp}$. Y can be calculated using the retrograde liquid volume data determined from PVT studies. The term S_{clh} is the critical hydrocarbon liquid saturation to reach equilibrium, or mobil liquid saturation. The other pertinent units are Mscfd, cps., days, ft. and Darcy.

The definition of skin effect (s) in terms of the radius of an altered zone r_a (equilibrium two-phase flow region), and the reduced permeability of the altered zone k_a , can be expressed as

$$s = \frac{(k - k_a)}{2k_a} \ln \left(\frac{r_a}{r_w} \right) \dots (17)$$

Substituting Eq. 16 into 17 we obtain

$$s(q,t) = \frac{(k - k_a)}{2k_a} \ln \left[\frac{.1135 q_g^2 uZYt}{h^2 \phi k \bar{p} S_{clh} r_w^2} \right] \dots (18)$$

Equation 18 defines a rate and time dependent skin term that can give the appearance of non-Darcy flow. The equation, although approximate, gives a simple analytical expression with which to estimate the effects of two-phase flow in the vicinity of the wellbore. The significance of this effect in condensate wells has been demonstrated by others,^{14, 15, 16, 17}. Eq. 18 has been used to successfully analyze the results obtained from isochronal tests on condensate wells. A significant portion of the skin was attributed to $s(q,t)$.

s (q,t) FOR OIL WELLS

In the studies of West et al¹⁸, Perrine¹⁹ and Weller²⁰, an analogous behavior around the wellbore has been shown to exist in an oil well. Under constant rate production for initially saturated solution-gas drive reservoirs, their results show that the gas saturation quickly builds up to the equilibrium gas saturation (critical gas) and remains constant at its equilibrium value. Its' radius increases with time until the wells drainage volume is above the critical gas saturation. (See Fig. 4) This gas saturation build-up in the vicinity of the wellbore is commonly referred to as "gas block". The corresponding oil permeability reduction in this region is

therefore constant, with its radius increasing with time. This damaged zone within which the relative permeability has been reduced has been referred to as a pseudo-skin by Weller. Utilizing Eq. 18 with the appropriate variable substitution, the rate and time dependent skin $s(q,t)$ for an oil well is

$$s(q,t) = \frac{(k - k_a)}{2k_a} \ln \left[\frac{.0226 q_o^2 B_o u_o Xt}{h^2 \phi k S_{cg} r_w^2} \right] \dots (19)$$

where X is expressed as reservoir cubic feet of gas evolved in the reservoir per stock tank barrel of oil produced per psi, $\frac{dc}{dp}$. X is readily obtained from a standard PVT study using the liberated gas data R_L as a function of pressure. S_{cg} is the equilibrium or critical gas saturation, fraction of pore volume. Other pertinent units are STK BOPD, cps, DAY, FT, DARCY and RES BBL/STK BBL.

The results of West et al were first used to determine whether Eq. 19 would reasonably predict the radius of the "pseudo-skin" for times before boundary effects became significant. Using the basic data given in their paper and Eq. 19 a calculated $r_a = 1.6$ FT versus their 1.5 FT was obtained at 2.21 days, and $r_a = 4.6$ FT versus their 6.0 FT at 16.8 days.

Eqs. 18 or 19 are applicable to initially saturated and partially undersaturated reservoirs. Once an oil well's drainage volume exceeds the equilibrium gas saturation Eq. 19 is no longer applicable. For condensate wells, Eq. 18 will apply for a much longer period of time, at least until revaporization begins to take place. Then r_a will begin to recede.

Only in the case of undersaturated reservoirs, we could assume that the two-phase region is at the equilibrium gas saturation and exists out to where the pressure is equal to the bubble-point pressure. This simpler approach, developed by Handy²¹ for wells producing from undersaturated reservoirs, leads to the maximum reduction of PI which could be expected from a gas saturation build-up around a well producing with a flowing pressure below the bubble-point pressure. By analogy, the same approach could be used for treating undersaturated gas condensate wells.

For completeness then, Eqs. 12 and 13 should be written to include a rate and time dependent skin, $s(q,t)$. We would then have

$$\frac{7.08 kh (p_i - p_{wf})}{q (uB)} = \ln \sqrt{\frac{14.23 k_i t}{\phi (u c_t)_i r_w^2}} + s + s(q,t) + Dq \dots (20)$$

and

$$\frac{7.08 kh [m(p_i) - m(p_{wf})]^2}{q} = \ln \sqrt{\frac{14.23 k_i t}{\phi(u_{ct})_i r_w^2}} + s + s(q,t) + Dq \quad \dots (21)$$

After Ramey²², we can define

$$s' = s + Dq \quad \dots (22)$$

and

$$s'' = s + s(q,t) + Dq \quad \dots (23)$$

WELL TEST RESULTS

The basic results obtained from isochronal back-pressure tests and flow after flow multipoint tests conducted on oil wells are summarized in Tables 1 and 2.

Reservoir fluid states in which multipoint well tests were obtained are, in chronological order,

1. Gas saturation existed throughout the reservoir above the critical or equilibrium gas saturation.
2. Undersaturated reservoir with flowing pressures obtained both above and below the bubble-point pressure.
3. Saturated reservoirs with the reservoir pressure at or very near the bubble-point pressure.
4. Undersaturated reservoir with all flowing pressures above the bubble-point pressure.

GAS SATURATION ABOVE EQUILIBRIUM

Stabilized flow after flow multipoint back-pressure tests were available on 16 wells producing from a solution-gas drive carbonate reservoir, Field A. Reservoir conditions were ideal for testing the hypothesis that q_0 vs. $(\bar{p}_R^2 - p_{wf}^2)$ would plot as a straight line on log-log graph paper with a slope (n) of 1. The reservoir variables in this field closely approximated those used by Vogel in his study, (See Table 3). Average gas saturation in the reservoir at the time the tests were conducted was estimated to be between 10 or 12 percent. Producing gas-oil ratios when compared to the initial solution gas-oil ratio of 684 SCF/BBL indicates that the reservoir was well above the equilibrium (critical gas) saturation at the time the tests were conducted. Gas-oil ratios increased only moderately at increasing drawdowns for most tests.

Although the unit slope did predominate, four wells exhibited back-pressure curve slopes much less than 1. A slope less than 1 results in an even more rapid decline in rate q with drawdown than would be predicted from Vogel's IPR equation.

The test on Well 6, Field A (Fig. 5) consisted of seven individual flows, each to apparent stabilization. The first four flow rates were run in a normal increasing sequence. Following the fourth flow at 229 BOPD, the rate was reduced to 93 BOPD then again followed by an increasing sequence of flows. All points essentially fell on the same line, indicating that transient effects were not the cause of the deviation from the linear relationship predicted by the productivity index concept. Note that the flow points define a performance curve with a slope of 1 almost to its absolute open flow potential (AOFPP). Table 1 shows that for all wells tested in this field, the maximum flow rate was very near the extrapolated absolute open flow potential. In the other fields in which multipoint tests were conducted, equipment limitation precluded defining the entire curve, requiring a greater degree of extrapolation to AOFPP.

Well No. 3, Field A, (Fig. 6) illustrates the most significant result of this first group of tests. With an excellent alignment of five stabilized flows, the slope of the back-pressure curve is 0.648. The results obtained from this test first suggested the possible existence of the same lower limit of the exponent (n) as exists for gas wells ($n = 0.500$), and a non-Darcy flow effect.

Well No. 14, Field A, (Fig. 7) exhibited the maximum increase in gas-oil ratio with increasing drawdown of all the wells tested. Even with the gas-oil ratio increasing with rate, the slope n of the performance curve was 1.0.

UNDERSATURATED RESERVOIR ($p_{wf} > p_b$ and $p_{wf} < p_b$)

In an attempt to utilize the oil well back-pressure testing method to more accurately predict full development well performance from wildcat well tests, an isochronal test program was initiated. The first known oil well isochronal test was conducted on April 14, 1970 on the Phillips Ekofisk 2/4-2X well. Surprising results were obtained from these first tests. Two straight lines were obtained when a log q vs log $(\bar{p}_R^2 - p_{wf}^2)$ plot was prepared. Figure 8 illustrates the results obtained from a 6 hour isochronal test conducted on zone 2.

Handy's²¹ work led to the conclusion that the two straight lines were a result of the reservoir being undersaturated, with the intersection point indicating the apparent reservoir bubble-point pressure. Using the first two

flow rates and the constant PI approach, an apparent absolute open flow potential of 13,000 BOPD is indicated. The true potential established by extrapolation of drawdown data below the bubble-point pressure is 5200 BOPD. Calculated permeability from build-up data following the first single phase flow was 6.1 MD with a skin $s = 0$. For flows at pressure drawdowns below the bubble-point pressure, a rate dependent skin was indicated. The rate dependent skins extrapolated to a skin of 0 at the point single phase flow ended, $q_o \cong 2100$ BOPD, as should be expected, (See Fig. 9). Single-phase skins of -4 are normally obtained from tests following acid stimulations. This favorable response usually precluded obtaining drawdowns below the bubble-point pressure after acid because of equipment limitations. As a result, no after acid isochronal tests have been obtained which could demonstrate whether the nature of the performance curve is substantially different than that obtained before acid. Isochronal tests conducted on two other zones in this well, before stimulation, yielded similar results.

Starting with Eq. 8A, we can outline the procedure used to calculate the bubble-point pressure from the pre-acid test

$$q_o = J'_o (p_b^2 - p_{wf}^2) + J_o (p_e - p_b) \dots (8A)$$

If we then define

$$q(2) = J'_o (p_b^2 - p_{wf}^2) \dots (24)$$

$$\text{and } q(1) = J_o (p_e - p_b) \dots (25)$$

$$\text{then } q_o = q(2) + q(1) \dots (26)$$

(No physical significance should be attached to $q(1)$ or $q(2)$ since it is obvious that for the steady state assumption upon which it was derived, the total q_o must be flowing through both regions.)

When combined two-phase and single phase flow are occurring in a well

$$q(1) = \text{CONSTANT} = J_{o, p_e, F_b} (p_e - p_b) \dots (25)$$

therefore $q(2) = q_o$ (measured) - $q(1) =$

$$J'_o (p_b^2 - p_{wf}^2) \dots (27)$$

With the correct value of a bubble-point pressure, p_b , a plot of $q(2)$ vs. $(p_b^2 - p_{wf}^2)$ should plot a straight line on either cartesian or a log-log plot. On a log-log plot, the slope is 1.0 and the intercept J'_o .

The 1.0 slope was assumed for the two-phase term at this stage of development because of the computer results obtained by Vogel and the results obtained from tests in Field A. However, the fact that slopes less than 1.0 are indicated from other tests where two-phase flow existed in the reservoir, suggests the more general form of Eq. 8A to be

$$q_o = J'_o (p_b^2 - p_{wf}^2)^n + J_o (p_e - p_b) \dots (28)$$

A trial and error calculation assuming various values of p_b was performed until a slope of 1 was obtained, (See Fig. 10). This resulted in a calculated bubble-point pressure of 5874 psia. A bubble-point pressure of 5885 psia was determined from a PVT study of the reservoir fluid obtained from this well.

A simple graphical estimate of the bubble-point pressure from the apparent intersection point is probably adequate because of the uncertainties introduced by n , the exponent of the two-phase term, being a variable. Once the true bubble-point pressure is determined from PVT data, n can be directly calculated.

SATURATED RESERVOIRS

Most of the reservoirs in Fields C thru H are saturated at initial reservoir pressure. The reservoirs are very similar in nature at corresponding depths since the fields are in close proximity to each other. All reservoirs are relatively clean Tertiary sandstones ranging in depth of from 7800 to 11200 feet. Permeabilities determined from build-up tests ranged from 130 to 2500 MD with net pays ranging from 20 to 180 feet in thickness. Typical porosities are 22 percent with water saturations of around 30 percent. Relative permeability measurements exhibited critical gas saturations ranging from 7 to 13 percent.

Humping effects, wellbore storage, flat pressure build-up curves and the short duration of the build-ups made the determination of permeabilities difficult on several wells. For those wells not having permeabilities listed in the tables, its order of magnitude is reflected by the wells AOF. A summary of all the isochronal test results obtained appear in Table 2.

The standard isochronal test in these fields consisted of a four hour flow followed by a four hour shut-in. Occasionally a flow after flow test was also conducted. Increasing and decreasing sequences of flows were performed on most tests to check reproductability. Because of the rather high permeabilities in these reservoirs, flow after flow tests often duplicated the isochronal test performance

curve. Performance curve slopes obtained from these tests are seen to range from 0.568 to 0.875. Not one single well exhibited the 1 slope that was so predominant in Field A. Several of the well test performance curves obtained in initially saturated reservoirs are shown in Figs. 11 - 21. In general, flow point alignment to establish an oil wells performance curve is as good as that obtained from gas well back-pressure tests. Shut-in pressure recovery between isochronal flows on these tests is sufficient to establish true isochronal conditions. Gas-oil ratio variations are considered to be more a function of separator pressure than reservoir drawdown pressure effects. The most significant observation to be made from these tests is that flow after flow data fall on the same performance curve as that established by isochronal data points. The lowest permeability of this group of wells is 130 MD. Test results for Well No. 3-C, Field C, (Fig. 12 and Table 4) demonstrate the flow after flow and isochronal test performance curve reproducibility by two separate tests conducted one week apart.

The test on Well No. 5-C in Field D was selected to apply Eq. 20 to analyze the well performance data. The four hour isochronal well performance curve was established by two separate tests six months apart. Nearly 100 psi reservoir pressure drop occurred between these two tests. No detectable shift in the position of the well's performance curve was noted. Well No. 5-C was the only one of the saturated reservoir wells that had a fully perforated interval, thus eliminating yet another variable, partial penetration effects. Further, the permeability calculated from build-up data was consistent with measured core permeabilities for this well. Tables 5 and 6 summarize the reservoir and test data used in the calculations and the results obtained. The rate dependent skin term $s(q,t)$, for this well, was found to be insignificant at even the highest flowrate of 2308 BOPD. Both s' and s'' were plotted as a function of q_0 . In either case, a line can be drawn thru the plotted points to $q = 0$ yielding a formation skin $s = 0$. Non-Darcy flow appears to be significant for this well.

The isochronal performance curve obtained on Well No. 7-e, Field D, (Fig. 16), exhibits the steepest slope of all the tests conducted in a saturated reservoir. Any of the flow rates would be reasonable for a normal single flow drillstem test. A comparison of calculated absolute open flow potential (AOFPP) is made using the PI method and Vogel's IPR method for each of the flow rates. The maximum error in AOFPP is of course obtained with the lowest flow rate - AOFPP = 57,200 BOPD PI method, 31,990 BOPD IPR method and actual isochronal AOFPP = 7250 BOPD. Eventhough the error in AOFPP, using

the PI or IPR methods is reduced when determined at the highest flow rate, the error in evaluating skin and flow efficiency will be increased.

Well No. 8-e, Field D, (Fig. 17 and Table 7) demonstrates the change in the wells performance curve as a result of increasing the perforated interval from 20 Ft. to 60 Ft.; net pay is 182 Ft. The wells potential nearly doubled and the slope of the performance curve increased only slightly.

UNDERSATURATED RESERVOIR ($p_{wf} > p_b$)

Of all the isochronal tests conducted, the most surprising results were those obtained on Wells 1-a and 2-b in Field G (Figs. 22 and 24 respectively). With all flowing pressures well above the reservoir bubble-point pressure, (single-phase liquid flow), slopes of 0.813 and 0.712 were obtained from a $\log q$ vs. $\log \Delta(p^2)$ plot.

Conclusive evidence of the occurrence of non-Darcy flow in an oil well is demonstrated from a detailed analysis of the isochronal test data obtained on Well No. 1-a. PVT studies conducted on two bottom-hole samples and a recombination of surface samples indicated bubble-point pressures of 4495, 4756 and 4785 psia respectively. The lowest flowing pressure obtained on this test was 5669 psia at a flow rate of 2973 STK BOPD. Net pay for this well is 25 feet with a perforated interval of 10 feet.

The isochronal performance curve for Well No. 1-a (Fig. 22) indicates a slope n of 0.813 with an excellent alignment of 8 separate flow rates. Three decreasing sequence flows were followed by five more decreasing flows. Table 8 summarizes the data obtained for each flow rate. The fact that alignment was obtained following repeated flows and shut-ins, and flow reversals tends to indicate that a pressure dependent permeability would not account for the non-linear flow behaviour²³. The normal hysteresis effect^{24,25} in a pressure dependent permeability caused by repeated pressure reversals, as occurred during this isochronal test, should not have allowed the flows to retrace the back-pressure curve.

Analyses performed on build-ups obtained after four of the flows yielded consistent permeabilities of 222 MD. The skin effect calculated from these build-up analyses was found to be rate dependent. When s was plotted as a function of q , a skin at $q = 0$ of +2.2 and a non-Darcy flow coefficient $D_0 = .00233 \text{ BOPD}^{-1}$ was obtained (Fig. 23). From Reference²⁶, a partial penetration skin s_b was calculated to be +2.5, in very close

agreement with that obtained extrapolating to $q_o = 0$. The reservoir skin damage (s) therefore is concluded to be 0.

A further verification of non-Darcy flow in this well was made by checking the Reynolds number

$$R_e = \frac{\rho v d}{\mu} \dots \dots \dots (29)$$

A Reynolds number of 8 was obtained for the well under its flowing condition of 2973 BOPD with a flash formation volume factor of 2.70, a density of 0.48 gm/cc, 0.22 cps. viscosity, and assuming a grain diameter of 0.5 mm. According to Muskat¹² turbulent flow can be expected for Reynolds numbers greater than 1.

The necessity for conducting multi-rate tests on oil wells for the correct evaluation of well performance, PI, reservoir damage, flow efficiency and potential is particularly emphasized by this example. One can also conclude that non-Darcy flow would also exist in the presence of a gas saturation around the wellbore and would be even more severe than is indicated for the single phase liquid flows. For Well No. 1-a, a break in the performance curve should occur for flows below the bubble-point pressure, with the absolute open flow potential being even less than that indicated by the extrapolation on Fig. 22.

CHANGE IN PERFORMANCE CURVES WITH DEPLETION

Perhaps the biggest impediment to an earlier development of multipoint testing of oil wells was the realization that a well's performance curve changes with changing oil saturation and pressure in a complex manner. Standing²⁷ extended the utility of Vogel's IPR equation (performance curve) by illustrating a simple method to correct a known IPR curve position to some future position as a result of a change in k_{ro} . The future value of k_{ro} in $\frac{k_{ro}}{u_{Bo}}$

his example was obtained from a Turner material balance calculation using a Corey-type correlation for k_{ro} . The inability to define a real k_{ro} curve for a specific well still makes this approach only approximate.

It has been observed that in many material balance calculations for solution-gas drive reservoirs, k_{ro} is approximately linear with reservoir pressure. As an approximation to the change in oil permeability with pressure depletion we could then write

$$\frac{k(\bar{p}_R)}{k_i} = \frac{\bar{p}_R}{\bar{p}_{Ri}} \dots \dots \dots (30)$$

or

$$k_{ro}(\bar{p}_R) = \frac{\bar{p}_R}{\bar{p}_{Ri}} \dots \dots \dots (31)$$

where k_{ro} is with respect to k_i and is defined at a vanishing Δp , zero drawdown. \bar{p}_{Ri} is also assumed to be equal to or less than the bubble-point pressure. Then $k_{ro}(\bar{p}_R)$ plotted $\frac{k_{ro}(\bar{p}_R)}{(u_{Bo})_{pR}}$

as a function of pressure defines a locus of values at zero drawdown. Using Eq. 10 to define drawdown and Eq. 31 to correct for depletion we obtain a simple empirical equation to predict the flow rate q_o for both drawdown and reservoir pressure depletion.

$$q_o = J'_{oi} \left(\frac{\bar{p}_R}{\bar{p}_{Ri}} \right) (\bar{p}_R^2 - p_{wf}^2) \dots \dots (32)$$

The subscript i defines any arbitrary initial condition at or below bubble-point pressure.

Equation 32 was tested using the results shown in Vogel's Figure 7. A comparison of his results with that using Eq. 32 is given in tabular and graphical form on Fig. 25. The pressure ratio correction was also applied to results published in Ref. 28 with good results, (See Table 9). J'_{oi} was determined using both basic reservoir variables and an initial reported flow with about equal success. No field data exist at this time with which to check the above relationship, or the more general form

$$q_o = J'_{oi} \left(\frac{\bar{p}_R}{\bar{p}_{Ri}} \right) (\bar{p}_R^2 - p_{wf}^2)^n \dots \dots (33)$$

suggested by the results of the multipoint tests conducted to date. Well No. 5-C in Field D developed a 100 psi decline in reservoir pressure between the two isochronal tests conducted six months apart. With or without the pressure ratio correction, the performance curves are essentially the same.

Fig. 26 graphically illustrates the various stages of the pressure function $\frac{k_{ro}}{(u_{Bo})}$ under

the conditions of pressure depletion and drawdown. Pertinent comments are included on the figure.

DISCUSSION

The forty multipoint tests reported in this study, isochronal and flow after flow, cover a wide range of reservoir fluids, fluid states, and reservoir variables. Vogel's computer study of inflow performance using two-phase flow theory covered a wide range of fluid

properties and relative permeability relationships. The combined results of theoretical and field studies indicate that multipoint tests are as necessary for oil wells as for gas wells. The fact that non-Darcy flow effects was found to be significant in field tests suggests that future theoretical computer studies need to include a non-Darcy flow effect. The exact nature of the non-Darcy flow and Reynolds number for two-phase flow in terms of reservoir and fluid variables needs further investigation.

To the author's knowledge, none of the wells included in this study were hydraulically fractured, true radial flow was obtained. Further field tests are needed to study the performance curves of fractured wells. They can be dominated by linear flow in the vicinity of the wellbore, the region in which non-Darcy flow should be most pronounced. West et al.¹⁸ in their study of linear and radial two-phase flow point out that "The linear system does not exhibit the constriction effects which were observed in the radial system." However, since gas well and oil well tests have been shown to exhibit similar behaviour and a significant number of tests on hydraulically fractured gas wells have been conducted without a breakdown in the $\log q$ vs. $\log \Delta(p^2)$ relationship, no real departure is expected for tests conducted in hydraulically fractured oil wells.

All tests reported in this study were taken at essentially one pressure level. A change in slope of the portion of the back-pressure curve, consisting of all flows at drawdowns below the bubble-point pressure, can be predicted with reservoir shut-in pressure decline to the bubble-point pressure for undersaturated reservoirs. Vogel's computer results (not including a non-Darcy flow effect) suggested a simple empirical reservoir shut-in pressure ratio factor to establish a single performance curve for both drawdown and pressure depletion for a volumetric reservoir without fluid injection. The nature of the change in the well performance curve with pressure depletion requires field study.

CONCLUSIONS

The results obtained from the forty oil well multipoint back-pressure tests reported in this study, isochronal and flow after flow, leads to the following conclusions:

1. Multipoint tests for oil wells are required to accurately determine flow rates as a function of drawdown, reservoir damage, flow efficiency, and a well's true absolute open-flow potential.

2. Oil wells can behave very similar to gas wells on multipoint back-pressure tests and should therefore be tested and analyzed using the same basic flow equations.

3. The exponent (n) for oil well tests determined from a $\log q$ vs. $\log \Delta(p^2)$ plot was found to lie between 0.568 and 1.000, very near the limits commonly accepted for gas well back-pressure curves.

4. Flow-point alignment to establish an oil well back-pressure curve on a $\log q$ vs. $\log \Delta(p^2)$ plot is as good as that normally obtained from gas well back-pressure tests.

5. A non-Darcy flow-term is generally required to account for slopes (n) less than 1 obtained on oil well back-pressure performance curves.

6. Back-pressure curve slopes less than 1 can be obtained on wells in undersaturated reservoirs without a non-Darcy flow term because of the shape of the pressure function ($k_{ro}/u_o B_o$).

7. In some cases, it is possible to determine the bubble-point pressure of an undersaturated reservoir from multipoint tests when a sufficient range of flow rates is taken.

8. Flow after flow tests or isochronal tests on oil wells will yield the same performance curve in high permeability reservoirs.

9. With a single data point, a simple empirical equation predicts flow rates as a function of drawdown and pressure depletion for wells in a volumetric solution-gas drive reservoir, (no fluid injection). Field verification is obviously needed.

NOMENCLATURE

- a = slope of pressure function $f(p)$,
(psi - cp.)⁻¹
- b = intercept of pressure function $f(p)$,
cp.⁻¹
- B = formation volume factor, reservoir vol./
surface vol.
- c_t = total compressibility, psi⁻¹
- C = back-pressure curve coefficient
- D = non-Darcy flow constant, (STK BOPD)⁻¹
- h = thickness, ft.
- J = productivity index, STK/BBL/DAY/psi
- J' = productivity index (back-pressure curve
coefficient) STK/BBL/DAY/(psi)²ⁿ
- k = effective permeability, Darcy
- k_a = permeability of altered or damaged zone,
Darcy
- k_{ro} = relative permeability to oil, fraction
- m(p) = pseudo-pressure, (See Eq. 14), psi/cp.

| | |
|-------------|--|
| n | = exponent of back-pressure curve |
| \bar{p} | = average pressure, psia |
| p_b | = bubble point pressure, psia |
| p_e | = external boundary pressure, psia |
| \bar{P}_R | = reservoir average pressure (shut-in pressure), psia |
| p_i | = initial formation pressure, psia |
| p_{wf} | = bottom-hole flowing pressure, psia |
| PI | = productivity index (J), STK BBL/DAY/PSI |
| q | = surface rate of flow, STK BOPD |
| r_a | = radius of altered or damaged zone, ft. |
| r_e | = external boundary radius, ft. |
| r_w | = wellbore radius, ft. |
| R_L | = Gas-oil ratio liberated per barrel of residual oil, SCF/STK BBL |
| s | = skin effect, dimensionless |
| s_b | = skin effect caused by partial penetration of formation, dimensionless |
| s' | = total effective skin effect (see Eq. 22), dimensionless |
| s'' | = total effective skin effect (see Eq. 23), dimensionless |
| $s(q,t)$ | = rate and time dependent skin effect (see Eqs. 18 and 19) dimensionless |
| S | = saturation, fraction of pore volume |
| S_{clh} | = hydrocarbon liquid saturation to achieve mobility, fraction of pore volume |
| t | = time, days |
| T | = reservoir temperature, °R |
| X | = reservoir cu. ft. of gas evolved in the reservoir/STK BBL produced/psi, (dc/dp) in Eq. 15 |
| Y | = reservoir cu. ft. of condensate accumulation in the reservoir/MSCF full wellstream gas produced/psi, (dc/dp) in Eq. 15 |
| z | = gas deviation factor, dimensionless |
| u | = viscosity, cp. |
| ϕ | = porosity, fraction of bulk volume |

SUBSCRIPTS

| | |
|-----|-----------|
| i | = initial |
| o | = oil |
| g | = gas |

ACKNOWLEDGMENTS

I wish to thank Phillips Petroleum Co. for permission to publish this paper. The support and assistance of numerous people in our International Department is gratefully acknowledged.

REFERENCES

1. Rawlins, E. L., and Schellhardt, M. A., "Back-Pressure Data on Natural Gas Wells and Their Application to Production Practices", U.S. Bureau of Mines Monograph 7, 1936.
2. Cullender, M. H.: "The Isochronal Performance Method of Determining the Flow Characteristics of Gas Wells", Trans. AIME (1955) 204, 137.
3. Moore, T. V.: "Determination of Potential Production of Wells without Open Flow Test", API Production Bulletin 206, (1930), 27.
4. Evinger, H. H. and Muskat, M.: "Calculation of Theoretical Productivity Factor", Trans. AIME (1942) 146, 126.
5. Vogel, J. V.: "Inflow Performance Relationships for Solution-Gas Drive Wells", J. Pet. Tech. (Jan., 1968), 83.
6. Rowan, G. and Clegg, M. W.: "An Approximate Method for Non-Darcy Radial Gas Flow", Soc. Pet. Eng. J. (June, 1964), 96.
7. Smith, R. V.: "Unsteady-State Gas Flow into Gas Wells", J. Pet. Tech. (Nov., 1961), 1151.
8. Swift, G. W. and Kiel, O. G.: "The Prediction of Gas Well Performance Including the Effect of Non-Darcy Flow", J. Pet. Tech. (July, 1962) 791.
9. Al-Hussainy, R. and Ramey, H. J., Jr.: "Application of Real Gas Flow Theory to Well Testing and Deliverability Forecasting", J. Pet. Tech. (May, 1966) 637.
10. Al-Hussainy, R., Ramey, H. J., Jr. and Crawford, P. B.: "The Flow of Real Gases Through Porous Media", J. Pet. Tech. (May, 1966) 624.
11. Raghavan, R., Scorer, J. D. T. and Miller, F. G.: "An Investigation by Numerical Methods of the Effect of Pressure-Dependent Rock and Fluid Properties on Well Flow Tests", Soc. Pet. Eng. J. (June, 1972), 267.

12. Muskat, M.: Physical Principles of Oil Production, McGraw-Hill Book Co., Inc., New York (1949) 793, 126.
13. Muskat, M.: "Some Theoretical Aspects of Cycling-Part 2, Retrograde Condensation About Well Bores", Oil & Gas Journal, Reprint (Circa 1950).
14. Eilerts, C. K. et al: "Integration of Partial Differential Equations for Transient Radial Flow of Gas-Condensate Fluids in Porous Structures", Soc. Pet. Eng. J. (June 1965) 141.
15. Gondouin, M., Iffly, R. and Husson, J.: "An Attempt to Predict the Time Dependence of Well Deliverability in Gas Condensate Fields", Soc. Pet. Eng. J. (June, 1967) 113.
16. O'Dell, H. G. and Miller, R. N.: "Successfully Cycling A Low Permeability, High-Yield Gas Condensate Reservoir", J. Pet. Tech. (Jan., 1967) 41.
17. Fussell, D. D.: "Single-Well Performance Predictions for Gas Condensate Reservoirs", Paper SPE 4072 Presented at the 47th Annual Fall Meeting, San Antonio, Texas, (Oct. 8-11, 1972).
18. West, W. J., Garvin, W. W. and Sheldon, J. W.: "Solution of the Equations of Unsteady-State Two-Phase Flow in Oil Reservoirs", Trans., AIME (1954) 201, 217.
19. Perrine, R. L.: "Analysis of Pressure-Buildup Curves", Drilling and Prod. Practice, API (1956) 482.
20. Weller, W. T., "Reservoir Performance During Two-Phase Flow", J. Pet. Tech. (Feb., 1966) 240.
21. Handy, L. L.: "Effect of Local High Gas Saturations on Productivity Indices", Drilling and Prod. Practice, API (1957) 111.
22. Ramey, H. J., Jr.: "Non-Darcy Flow and Wellbore Storage Effects in Pressure Build-up and Drawdown of Gas Wells", J. Pet. Tech. (Feb., 1965) 223.
23. Vairogs, J. and Vaughan, W. R.: "Pressure Transient Tests in Formations Having Stress-Sensitive Permeability", Paper SPE 4050 Presented at the 47th Annual Fall Meeting, San Antonio, Texas, (Oct. 8-11, 1972).
24. McLatchie, L. S., Hemstock, R. A. and Young, J. W.: "Effective Compressibility of Reservoir Rocks and Its Effects on Permeability", Trans. AIME (1958) 213, 386.
25. Vairogs, J., Hearn, C. L., Dareing, D. W. and Rhoades, V. W.: "Effect of Rock Stress on Gas Production from Low-Permeability Reservoirs", J. Pet. Tech. (Sept., 1971) 1161.
26. Brons, F. and Marting, V. E. "The Effect of Restricted Fluid Entry on Well Productivity", J. Pet. Tech. (Feb., 1961) 172.
27. Standing, M. B.: "Concerning the Calculation of Inflow Performance of Wells Producing from Solution Gas Drive Reservoirs", J. Pet. Tech. (Sept., 1971) 1141.
28. Levine, J. S. and Prats, M.: "The Calculated Performance of Solution-Gas-Drive Reservoirs", Soc. Pet. Eng. J. (Sept., 1961) 142.

APPENDIX

Equation 6

$$q_o = \frac{7.08 kh}{\left[\ln \left(\frac{r_e}{r_w} \right) + s' \right]}$$

$$\cdot \left[\int_{P_{wf}}^{P_b} \frac{k_{ro}(S,p) dp}{u_o B_o} + \frac{(p_e - p_b)}{(u_o B_o)} \right] \dots (6)$$

can be used to describe all three possible flow conditions that could exist for a producing well at some time during the life of an initially undersaturated oil reservoir by eliminating any terms that do not apply over appropriate pressure ranges.

I Single-Phase Flow: $p_{wf} > p_b$, $p_e > p_b$ or $\bar{p}_R > p_b$

A. STEADY-STATE FLOW, Constant Pressure at Outer Boundary

$$q_o = \frac{7.08 kh}{\left[\ln \left(\frac{r_e}{r_w} \right) + s' \right]} \left[\frac{(p_e - p_{wf})}{(u_o B_o)} \right] \dots (A-1)$$

B. PSEUDO-STEADY STATE FLOW, Closed (NO FLOW) at Outer Boundary

a) Boundary Pressure p_e is known at r_e (Initial Isochronal e Test)

$$q_o = \frac{7.08 kh (p_e - p_{wf})}{\left[\ln \left(\frac{r_e}{r_w} \right) - \frac{1}{2} + s' \right] (u_o B_o)} \dots (A-2)$$

b) Average pressure \bar{p}_R is known ($\bar{p}_R =$ shut-in pressure)

$$q_o = \frac{7.08 kh (\bar{p}_R - p_{wf})}{\left[\ln \left(\frac{r_e}{r_w} \right) - \frac{3}{4} + s' \right] (u_o B_o)} \dots (A-3)$$

c) TRANSIENT FLOW

$$q_o = \frac{7.08 kh (p_i - p_{wf})}{\left[\ln \sqrt{\frac{14.23 k_i t}{\phi (u c_t)_i r_w^2}} + s' \right] (u_o B_o)} \dots (A-4)$$

II Two-Phase Flow: $p_{wf} < p_b, p_e \leq p_b$ or $\bar{p}_R \leq p_b$, and

$$S_g > S_{gc}$$

A. STEADY-STATE FLOW [Constant Pressure at Outer Boundary]

$$q_o = \frac{7.08 kh}{\left[\ln \left(\frac{r_e}{r_w} \right) + s' \right]} \int_{p_{wf}}^{p_e} \frac{k_{ro}(S,p)}{u_o B_o} dp \dots (A-5)$$

B. PSEUDO-STEADY STATE FLOW [Closed (No Flow) at Outer Boundary]

a) Boundary Pressure p_e is known at r_e (Initial Isochronal Test)

$$q_o = \frac{7.08 kh}{\left[\ln \left(\frac{r_e}{r_w} \right) - \frac{1}{2} + s' \right]} \int_{p_{wf}}^{p_e} \frac{k_{ro}(S,p)}{u_o B_o} dp \dots (A-6)$$

b) Average Pressure \bar{p}_R is known ($\bar{p}_R =$ Shut-in pressure)

$$q_o = \frac{7.08 kh}{\left[\ln \left(\frac{r_e}{r_w} \right) - \frac{3}{4} + s' \right]} \int_{p_{wf}}^{\bar{p}_R} \frac{k_{ro}(S,p)}{u_o B_o} dp \dots (A-7)$$

C. TRANSIENT FLOW

$$q_o = \frac{7.08 kh}{\left[\ln \sqrt{\frac{14.23 k_i t}{\phi (u c_t)_i r_w^2}} + s' \right]} \int_{p_{wf}}^{p_i} \frac{k_{ro}(S,p)}{u_o B_o} dp \dots (A-8)$$

III Two-Phase and Single-Phase Flow:

$$p_{wf} < p_b, p_e > p_b \text{ or } \bar{p}_R > p_b$$

A. STEADY-STATE FLOW (Constant Pressure at Outer Boundary)

$$q_o = \frac{7.08 kh}{\left[\ln \left(\frac{r_e}{r_w} \right) + s' \right]} \left[\int_{p_{wf}}^{p_b} \frac{k_{ro}(S,p)}{u_o B_o} dp + \frac{(p_e - p_b)}{(u_o B_o)_{p_e, p_b}} \right] \dots (A-9)$$

B. PSEUDO-STEADY STATE FLOW (Closed (No flow) at Outer Boundary)

a) Boundary Pressure p_e is known at r_e (initial isochronal test)

$$q_o = \frac{7.08 kh}{\left[\ln \left(\frac{r_e}{r_w} \right) - \frac{1}{2} + s' \right]} \left[\int_{p_{wf}}^{p_b} \frac{k_{ro}(S,p)}{u_o B_o} dp + \frac{(p_e - p_b)}{(u_o B_o)_{p_e, p_b}} \right] \dots (A-10)$$

b) Average Pressure \bar{p}_R is known ($\bar{p}_R =$ Shut-in pressure during depletion)

$$q_o = \frac{7.08 kh}{\left[\ln \left(\frac{r_e}{r_w} \right) - \frac{3}{4} + s' \right]} \left[\int_{p_{wf}}^{p_b} \frac{k_{ro}(S,p)}{u_o B_o} dp + \frac{(\bar{p}_R - p_b)}{(u_o B_o)_{\bar{p}_R, p_b}} \right] \dots (A-11)$$

C. TRANSIENT FLOW

$$q_o = \frac{7.08 kh}{\left[\ln \sqrt{\frac{14.23 k_i t}{\phi (u c_t)_i r_w^2}} + s' \right]} \left[\int_{p_{wf}}^{p_b} \frac{k_{ro}(S,p)}{u_o B_o} dp + \frac{(p_i - p_b)}{(u_o B_o)_{p_i, p_b}} \right] \dots (A-12)$$

All of the preceding flow equations could be more simply expressed in terms of a pseudo-pressure $m_o(p)$

where $\int_{p_{wf}}^{p_e} \frac{k_{ro}(s,p)}{u_o B_o} dp =$

$$\int_0^{p_e} \frac{k_{ro}(S,p)}{u_o B_o} dp - \int_0^{p_{wf}} \frac{k_{ro}(S,p)}{u_o B_o} dp \dots (A-13)$$

or
$$\int_{p_{wf}}^{p_e} \frac{k_{ro}(S,p)}{u_o B_o} dp = m_o(p_e) - m_o(p_{wf}) \dots (A-14)$$

For the limiting case of at least using known PVT properties ($u_o B_o$), — (assuming $k_{ro}(S,p) = 1$) we have

$$m_o(p_e) - m_o(p_{wf}) = \frac{p_b - p_{wf}}{(u_o B_o)_{p_b, p_{wf}}} + \frac{p_e - p_b}{(u_o B_o)_{p_e, p_b}} = \frac{p_e - p_{wf}}{(u_o B_o)_{avg}} \dots (A-15)$$

Note that $(u_o B_o)$ normally evaluated at the average pressure $(p_e + p_{wf})/2$ would not result in a properly weighted average. But for the decline in $k_{ro}(S,p)$, a plot of q_o vs $(p_e - p_{wf}) / (u_o B_o)_{avg}$ would plot a straight line with a slope of $7.08 kh / [\ln(\frac{r_e}{r_w}) + s']$ and intercept 0.

Let us now consider the case where $k_{ro}(S,p)$ decreases with increased drawdown, k_{ro} should approach 0, resulting in $k_{ro} / (u_o B_o)$ approaching 0. Assuming $k_{ro} / (u_o B_o)$ could be approximated by straight line functions as depicted in Fig. 2, we could write for the two-phase region.

$$\int_{p_{wf}}^{p_b} f(p) dp = \int_{p_{wf}}^{p_b} [a_2 p + b_2] dp \dots (A-16)$$

which when integrated between limits yields

$$\int_{p_{wf}}^{p_b} f(p) dp = \frac{a_2}{2} (p_b^2 - p_{wf}^2) + b_2 (p_b - p_{wf}) \dots (A-17)$$

To approximate Vogel's IPR equation we set $b_2 = 0$, then

$$\int_{p_{wf}}^{p_b} f(p) dp = \frac{a_2}{2} (p_b^2 - p_{wf}^2) \dots (A-18)$$

Replacing p_b with \bar{p}_R for the two-phase flow equation ($p_R \leq p_b$), we have

$$q_o = \frac{7.08 kh}{[\ln(\frac{r_e}{r_w}) + s']} \left[\frac{a_2}{2} (\bar{p}_R^2 - p_{wf}^2) \right] \dots (A-19)$$

The slope a_2 , for $b_2 = 0$, is simply $(k_{ro} / u_o B_o) / \bar{p}_R$. We then can write

$$q_o = \frac{7.08 kh}{[\ln(\frac{r_e}{r_w}) + s']}$$

$$\cdot \left[\left(\frac{k_{ro}}{u_o B_o} \right)_{\bar{p}_R} \frac{(\bar{p}_R^2 - p_{wf}^2)}{2\bar{p}_R} \right] \dots (A-20)$$

Defining

$$J'_o = \frac{7.08 kh}{[\ln(\frac{r_e}{r_w}) + s']}$$

$$\cdot \left[\left(\frac{k_{ro}}{u_o B_o} \right)_{\bar{p}_R} \left(\frac{1}{2\bar{p}_R} \right) \right] \dots (A-21)$$

then

$$q_o = J'_o (\bar{p}_R^2 - p_{wf}^2) \dots (A-22)$$

Similarly treating the single-phase flow region as depicted in Fig. 2. ($p_{wf} \leq p_b$)

$$q_o = \frac{7.08 kh}{[\ln(\frac{r_e}{r_w}) + s']}$$

$$\cdot \left[b_1 (p_e - p_{wf}) - \frac{a_1}{2} (p_e^2 - p_{wf}^2) \right] \dots (A-23)$$

In terms of PI at a vanishing ΔP ,

$$\Delta p \rightarrow 0 \quad J_{o0} = \frac{7.08 kh}{[\ln(\frac{r_e}{r_w}) + s']} [b_1 - a_1 p_e] \dots (A-24)$$

where a_1 or b_1 , if $a_1 = 0$, is simply $(k_{ro} / u_o B_o)$ evaluated at p_e .

For the combined single-phase and two-phase flow case we can write

$$q_o = \frac{7.08 kh}{[\ln(\frac{r_e}{r_w}) + s'] (u_o \bar{B}_o)_{p_e, p_b}}$$

$$\cdot \left[\frac{(u_o \bar{B}_o)_{p_e, p_b} a_2 (p_b^2 - p_{wf}^2) + (p_e - p_b)}{2} \right] \quad (A-25)$$

where $(u_o \bar{B}_o)_{p_e, p_b}$ is evaluated at the average

pressure $(p_e + p_b)/2$.

In terms of PI definition

$$q_o = J_o (u_o \bar{B}_o)_{p_e, p_b} \left(\frac{a_2}{2}\right) (p_b^2 - p_{wf}^2) + J_o (p_e - p_b) \dots (A-26)$$

or

$$q_o = J_o' (p_b^2 - p_{wf}^2) + J_o (p_e - p_b) \dots (A-27)$$

TABLE 1 - FIELD A - CARBONATE RESERVOIR AT 5,100 FT AND 108°F, SUMMARY OF STABILIZED FLOW AFTERFLOW BACKPRESSURE TEST RESULTS. GAS SATURATION ABOVE CRITICAL OR EQUILIBRIUM GAS SATURATION. AVERAGE STABILIZATION TIME 48 HOURS, FLOWS IN INCREASING SEQUENCE.

| Well No. | Number Of Flows | Shut-In Pressure \bar{P}_R PSIA | Maximum Flow Rate | | | Back-Pressure Curve | |
|----------|-----------------|-----------------------------------|-------------------|---------------|-----------------|---------------------|-----------|
| | | | q_o STK BOPD | P_{wf} PSIA | GOR SCF/STK BBL | Slope n | AOFB BOPD |
| 1 | 5 | 1339 | 370 | 619 | 2745 | 1.000 | 420 |
| 2 | 5 | 1347 | 468 | 739 | 3102 | 0.875 | 670 |
| 3 | 5 | 1200 | 292 | 530 | 2572 | 0.648 | 340 |
| 4 | 5 | 1307 | 345 | 563 | 2181 | 1.000 | 425 |
| 5 | 5 | 1281 | 238 | 548 | 3571 | 1.000 | 310 |
| 6 | 7 | 1345 | 341 | 638 | 3945 | 1.000 | 445 |
| 7 | 5 | 1215 | 222 | 520 | 4485 | 0.771 | 275 |
| 8 | 4 | 881 | 116 | 375 | 2019 | 1.000 | 143 |
| 9 | 5 | 1159 | 202 | 436 | 3219 | 1.000 | 243 |
| 10 | 7 | 1430 | 261 | 491 | 1056 | 1.000 | 295 |
| 11 | 5 | 1284 | 126 | 395 | 4008 | 1.000 | 165 |
| 12 | 4 | 1474 | 321 | 578 | 1003 | 1.000 | 375 |
| 13 | 4 | 878 | 71 | 379 | 5979 | 0.707 | 83 |
| 14 | 4 | 1410 | 208 | 632 | 4607 | 1.000 | 260 |
| 15 | 5 | 1366 | 108 | 370 | 3805 | 1.000 | 123 |
| 16 | 5 | 1217 | 106 | 357 | 3397 | 1.000 | 110 |

TABLE 2 - FIELDS C THROUGH H (TERTIARY SANDSTONES). SUMMARY OF 4-HOUR ISOCHRONAL BACKPRESSURE TEST RESULTS, SATURATED AND UNDERSATURATED RESERVOIRS (NO STIMULATION)

| Field | | Number Of Flows (Tests) | Reservoir | | Shut-In Pressure PR PSIA | Maximum Flow Rate | | | Gravity °API | Back-Pressure Curve | | Reservoir Fluid | Net Pay Ft. | Perforations Ft. | Perm. K MD |
|----------|-----------|-------------------------|-----------|----------|--------------------------|-------------------------|----------------------|-----------------|--------------|---------------------|-----------|-----------------|-------------|------------------|---------------|
| Well No. | Reservoir | | Depth Ft | Temp. °F | | q _o STK BOFD | R _{wf} PSIA | GOR SCF/STK BBL | | Slope n | AOPF BOPD | | | | |
| Field C | | | | | | | | | | | | | | | |
| 1 | a | 4 | 8080 | 180 | 3535.3 | 2488 | 3451.6 | 588 | 37.3 | 0.813 | 30000 | 2905 B.P. | 90 | 37 | |
| 2 | b | 7 | 9100 | 204 | 3778.9 | 2530 | 2988.2 | 1363 | 45.0 | 0.832 | 5750 | saturated | 11 | 6 | 200 B.U. |
| 3 | c | 14 (2) | 9100 | 205 | 3926.2 | 2520 | 3192.1 | 1397 | 45.4 | 0.613 | 5000 | " | 32 | 8 | 180 B.U. |
| 4 | d | 6 | 10450 | 220 | 4342.8 | 2303 | 4167.2 | 1896 | 46.7 | 0.752 | 15700 | " | 82 | 75 | |
| 5 | e | 5 | 10600 | 220 | 4396.4 | 2022 | 4171.8 | 1900 | 44.2 | 0.644 | 9100 | " | 97 | 10 | 24.0 B.U. |
| Field D | | | | | | | | | | | | | | | |
| 1 | a | 6 | 7550 | 174 | 3187.4 | 2634 | 2676.7 | 1235 | 47.9 | 0.644 | 5900 | saturated | 41 | 20 | |
| 2 | b | 7 | 8300 | 194 | 3507.1 | 2993 | 3167.3 | 1516 | 45.3 | 0.580 | 8000 | " | 97 | 37 | |
| 3 | b | 7 | 8320 | 196 | 3763.9 | 2495 | 3593.0 | 1705 | 42.8 | 0.694 | 12500 | " | 58 | 26 | 450 Avg. Core |
| 4 | b | 7 | 8620 | 196 | 3486.4 | 3753 | 3346.0 | 1545 | 47.2 | 0.645 | 20000 | " | 92 | 74 | |
| 5 | c | 8 (2) | 8600 | 200 | 3695.5 | 2308 | 3539.0 | 1309 | 43.7 | 0.580 | 9800 | " | 20 | 20 | 24.70 B.U. |
| 6 | d | 5 (2) | 8700 | 200 | 3766.8 | 3236 | 3519.9 | 1431 | 43.8 | 0.792 | 16300 | " | 36 | 14 | 1600 B.U. |
| 7 | e | 5 | 8650 | 200 | 3913.0 | 3060 | 3448.0 | 1460 | 43.8 | 0.568 | 7250 | " | 52 | 18 | 470 B.U. |
| 8 | e | 7 | 8830 | 205 | 3948.6 | 2502 | 3776.5 | 1348 | 43.5 | 0.602 | 10700 | " | 182 | 20 | 130 B.U. |
| 8 | e | 5 | 8830 | 205 | 3899.2 | 2620 | 3823.3 | 1358 | 43.8 | 0.658 | 20300 | " | " | 60 | |
| 9 | e | 5 | 9000 | 205 | 3981.1 | 2321 | 3747.1 | 1367 | 42.8 | 0.613 | 8700 | saturated | 35 | 16 | 860 B.U. |
| Field E | | | | | | | | | | | | | | | |
| 1 | a | 9 | 8440 | 217 | 3695.3 | 3689 | 3375.1 | 1290 | 43.9 | 0.875 | 17600 | saturated | 80 | 38 | |
| Field F | | | | | | | | | | | | | | | |
| 1 | a | 7 | 7830 | 156 | 3420.2 | 2800 | 3097.5 | 418 | 25.5 | 0.596 | 7800 | saturated | 42 | 8 | |
| 2 | b | 5 | 8450 | 164 | 3693.8 | 3088 | 3433.9 | 575 | 29.8 | 0.628 | 10600 | " | 41 | 16 | |
| Field G | | | | | | | | | | | | | | | |
| 1 | a | 8 | 11200 | 238 | 6454.2 | 2973 | 5669.1 | 2670 | 47.8 | 0.813 | 9600 | 4765 B.P. | 25 | 10 | 222 B.U. |
| 2 | b | 7 | 11230 | 238 | 6477.6 | 3519 | 5956.3 | 2991 | 46.3 | 0.712 | 13300 | 5035 B.P. | 44 | 42 | |
| Field H | | | | | | | | | | | | | | | |
| 1 | a | 7 | 7940 | 174 | 3486.3 | 2626 | 3279.5 | 132 | 34.2 | 0.803 | 15000 | N.A. | 47 | 20 | |

TABLE 3 - COMPARISON OF RESERVOIR VARIABLES OF FIELD A WITH VOGEL'S⁵ HYPOTHETICAL SOLUTION GAS DRIVE RESERVOIR

| | Field A | Vogel's ⁵ Fig. 7 |
|-------------------|---------|-----------------------------|
| P _i | 2020 | 2130 |
| P _b | 2020 | 2130 |
| B _{oi} | 1.39 | 1.35 |
| 1/B _{gi} | 150 | 150 |
| u _{oi} | 0.86 | 1.0 |
| u _{gi} | 0.02 | 0.02 |
| S _{wc} | 11.5 | 19.4 |
| φ | 13.2 | 13.9 |
| h | 114 | 23.5 |
| k-MD | 31 | 20 |
| R _{si} | 684 | 600 |
| Spacing-Acres | 40 | 20 |

TABLE 4 - SUMMARY OF 4-HOUR FLOW AFTERFLOW AND ISOCHRONAL TEST RESULTS, OIL WELL 3-C, FIELD C

| Flow No. | Shut-In Pressure P_R -PSIG | Flowing Pressure P_{wf} -PSIG | q_o STK BOPD | GOR SCF/STK BBL | Separator Pressure PSIG |
|-------------------------------|------------------------------|---------------------------------|----------------|-----------------|-------------------------|
| Flow After Flow Test 11/28/71 | | | | | |
| 1 | 3908.2 | 3180.1 | 2518 | 1397 | 572 |
| 2 | | 3409.3 | 2064 | 1322 | 500 |
| 3 | | 3610.8 | 1535 | 1200 | 490 |
| 4 | | 3817.6 | 687 | 1607 | 290 |
| 5 | | 3636.5 | 1394 | 1478 | 300 |
| 6 | | 3834.5 | 711 | 1612 | 252 |
| 7 | | 3847.8 | 534 | 1512 | 262 |
| 8 | | 3177.4 | 2520 | 1397 | 572 |
| SI 7HR. | 3907.3 | | | | |
| Isochronal Test 12/5/71 | | | | | |
| 9 | 3907.1 | 3440.4 | 2077 | 1379 | 450 |
| 10 | N. A. | 3759.2 | 1064 | 1555 | 258 |
| 11 | 3905.2 | 3434.7 | 2010 | 1502 | 467 |
| 12 | 3898.6 | 3654.5 | 1390 | 1490 | 305 |
| 13 | 3897.9 | 3811.5 | 709 | 1538 | 230 |
| 14 | 3901.0 | 3681.2 | 440 | 1611 | 154 |

TABLE 5 - EXAMPLE CALCULATIONS OF S' AND S'' FOR SATURATED RESERVOIR, OIL WELL 5-C, FIELD D

Reservoir Data

$K = 2469$ MD, Build-up & Core Data.
 $K_a = 1284$ MD, $K_{ro} = 0.52$ at 10 percent critical gas saturation, S_{cg}
 $h = 20$ Ft.
 $\phi = 0.21$
 $S_{wc} = 0.32$
 $C_t = 25 \times 10^{-6}$ PSI⁻¹
 $r_w = 0.33$ Ft.
 $u_o = 0.27$ cps.
 $B_o = 1.94$ RES BBL/STK BBL
 $t = 0.167$ DAYS
 $X_o = 8.223 \times 10^{-3}$ RES FT³/STK BBL/PSI, FROM PVT DATA

Summary of Results

| q_o STK BOPD | (Eq. 19) $S(q, t)$ | S'' (Eq. 20) $[S+S(q, t) + Dq]$ | S' $[S + Dq]$ |
|----------------|--------------------|-----------------------------------|-----------------|
| 2308 | 1.67 | 36.6 | 34.9 |
| 1452 | 1.24 | 26.6 | 25.4 |
| 757 | 0.64 | 11.1 | 10.4 |

An S' or S'' versus q_o plot yields $S=0$ when extrapolated to $q=0$.

TABLE 6 - SUMMARY OF 4-HOUR ISOCHRONAL TESTS OF OIL WELL 5-C, FIELD D

| Flow No. | Shut-In Pressure P_R -PSIG | Flowing Pressure P_{wf} -PSIG | q_o STK BOPD | GOR SCF/STK BBL | Separator Pressure PSIG |
|-----------------------------|------------------------------|---------------------------------|----------------|-----------------|-------------------------|
| Isochronal Test of 12/23/71 | | | | | |
| 1 | 3680.8 | 3524.3 | 2308 | 1211 | 422 |
| 2 | 3672.1 | 3604.0 | 1452 | 1309 | 260 |
| 3 | 3670.5 | 3658.4 | 757 | 1375 | 139 |
| 4 | 3672.9 | 3665.8 | 419 | 1383 | 92 |
| SI 4HR. | 3672.9 | | | | |
| Isochronal Test of 6/10/72 | | | | | |
| 1 | 3583.9 | 3565.0 | 669 | 1406 | 115 |
| 2 | 3577.6 | 3535.1 | 1035 | 1333 | 160 |
| 3 | 3580.5 | 3513.7 | 1413 | 1357 | 215 |
| 4 | 3580.0 | 3430.9 | 2303 | 1217 | 370 |
| SI 4HR. | 3570.7 | | | | |

TABLE 7 - SUMMARY OF 4-HOUR ISOCHRONAL TESTS OF OIL WELL 8-e, FIELD D

| Flow No. | Shut-In Pressure P_R -PSIG | Flowing Pressure P_{wf} -PSIG | q_o STK BOPD | GOR SCF/STK BBL | Separator Pressure PSIG |
|------------------------------|------------------------------|---------------------------------|----------------|-----------------|-------------------------|
| 20 Ft Perforations, 12/14/71 | | | | | |
| 1 | 3934.0 | 3912.5 | 701 | 1452 | 160 |
| 2 | 3930.6 | 3759.4 | 2447 | 1369 | 480 |
| 3 | | 3852.8 | 1648 | 1383 | 350 |
| 4 | 3920.9 | 3761.8 | 2502 | 1348 | 480 |
| 5 | 3927.9 | 3835.5 | 1775 | 1476 | 350 |
| 6 | 3921.4 | 3901.4 | 787 | 1496 | 160 |
| 7 | 3913.5 | 3910.2 | 490 | 1413 | 170 |
| SI 4HR. | 3933.9 | | | | |
| 60 Ft Perforations 6/1/72 | | | | | |
| 1 | 3899.2 | 3820.8 | 2490 | 1418 | 462 |
| 2 | | 3884.3 | 766 | 1413 | 298 |
| 3 | 3897.9 | 3887.6 | 727 | 1503 | 167 |
| 4 | 3896.1 | 3854.7 | 1591 | 1483 | 280 |
| 5 | 3892.2 | 3808.6 | 2620 | 1358 | 456 |

TABLE 8 - SUMMARY OF 4-HOUR ISOCHRONAL TEST RESULTS OF OIL WELL 1-a, FIELD G

| Flow No. | Shut-In Pressure \bar{P}_R -PSIG | Flowing Pressure P_{wf} -PSIG | q_o STK BOPD | GOR SCF/STK BBL | Separator | |
|----------|------------------------------------|---------------------------------|----------------|-----------------|---------------|----------|
| | | | | | Pressure PSIG | Temp. °F |
| 1 | 6439.5 | 5654.4 | 2973 | 2670 | 405 | 107 |
| 2 | | 6148.4 | 1328 | 2615 | 310 | 84 |
| 3 | 6427.1 | 6301.6 | 722 | 2680 | 215 | 68 |
| 4 | 6432.8 | 5660.1 | 2871 | 2835 | 445 | 106 |
| 5 | 6427.0 | 5947.0 | 2120 | 2668 | 395 | 96 |
| 6 | 6427.1 | 6181.2 | 1236 | 2593 | 380 | 82 |
| 7 | 6428.1 | 6249.9 | 992 | 2683 | 285 | 72 |
| 8 | 6427.1 | 6320.1 | 665 | 2591 | 240 | 68 |

TABLE 9 - USE OF PRESSURE RATIO TO FORECAST RATE OF FLOW WITH PRESSURE DEPLETION²⁸

RESERVOIR DATA USED

$P_i = P_o = 2075$ psia; $\phi = 0.139$; $s_{wc} = 0.177$; $h = 23.5$ Ft; $r_w = 0.33$ ft; $r_e = 1053$ ft (80 acres); $\mu_{oi} = 0.99$ cp.; $B_{oi} = 1.33$ RES BBL/STK BBL; $k = 25$ and 2.5 MD; $S_{cg} = .02$ (assumed to be established rapidly), $k_{ro} = 0.444 @ S_{cg}$.

RESULTS

| \bar{P}_R | P_{wf} | \bar{P}_R^2 | P_{wf}^2 | $\frac{\bar{P}_R}{P_{Rd}}$ | $\bar{P}_R^2 - P_{wf}^2$ | q_o - STK BOPD | | After | |
|--|----------|---------------|-------------|----------------------------|--------------------------|------------------|--------|------------|--|
| psia | psia | (Thousands) | (Thousands) | $\frac{\bar{P}_R}{P_{Rd}}$ | (Thousands) | Ref. 28 | Eq. 22 | Eq. (A-21) | |
| 80 acres, $k = 25$ MD; $J'_{oi} = 0.03735$ and 0.03717 BOPD/(Thousand psia ²) | | | | | | | | | |
| 1708 | 65 | 2917 | 4 | 1.000 | 2913 | 108.8 | 108.8* | 108.3 | |
| 1377 | 65 | 1896 | 4 | .8062 | 1892 | 53.3 | 57.0 | 56.7 | |
| 1054 | 65 | 1111 | 4 | .6171 | 1107 | 24.6 | 25.5 | 25.4 | |
| 519 | 65 | 269 | 4 | .3039 | 265 | 5.12 | 3.0 | 3.0 | |
| 80 acres, $k = 2.5$ MD; $J'_{oi} = 0.004118$ and 0.003870 BOPD/(Thousand psia ²) | | | | | | | | | |
| 1778 | 65 | 3161 | 4 | 1.0000 | 3157 | 13.0 | 13.0* | 12.2 | |
| 1367 | 65 | 2455 | 4 | .8813 | 2451 | 7.88 | 8.90 | 8.36 | |
| 1297 | 65 | 1682 | 4 | .7295 | 1678 | 4.32 | 5.04 | 4.74 | |
| 1112 | 65 | 1237 | 4 | .6254 | 1233 | 2.82 | 3.18 | 2.99 | |
| 871 | 65 | 759 | 4 | .4899 | 755 | 1.54 | 1.52 | 1.43 | |

$$\text{Eq. 32, } q_o = J'_{oi} \left(\frac{\bar{P}_R}{P_{Rd}} \right) (\bar{P}_R^2 - P_{wf}^2) ; * J'_{oi} = \frac{q_{oi}}{(\bar{P}_{Ri}^2 - P_{wf}^2)}$$

$$J'_{oi} = \frac{7.08k (k_{ro})_{cg} h}{\left[\ln \left(\frac{r_e}{r_w} \right) - \frac{1}{2} \right] (u_o B_o)_i 2P_i} \cdot \frac{\bar{P}_{Ri}}{P_i} ; J'_{oi} \text{ at } \bar{P}_{Ri} \text{ of examples}$$

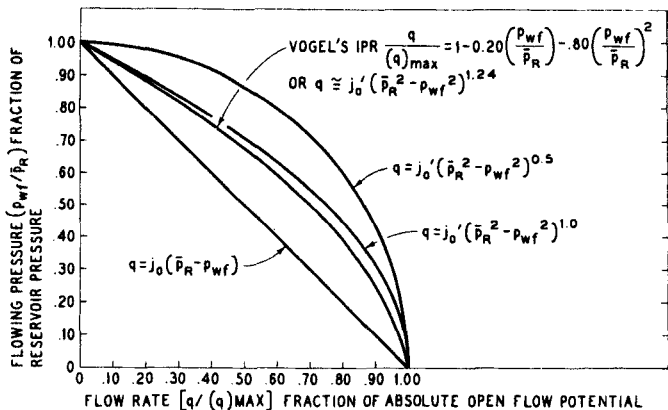


Fig. 1 - Inflow performance relationships for various flow equations.

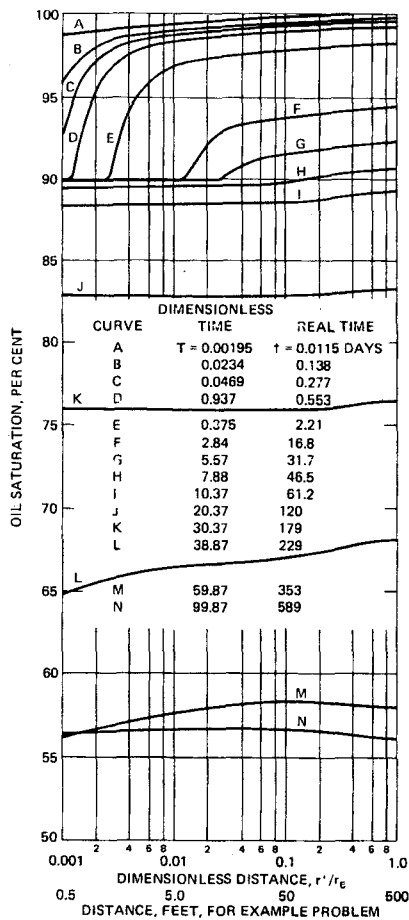


Fig. 4 - Calculated oil saturation profile history of a hypothetical solution, gas drive radial flow system.¹⁸

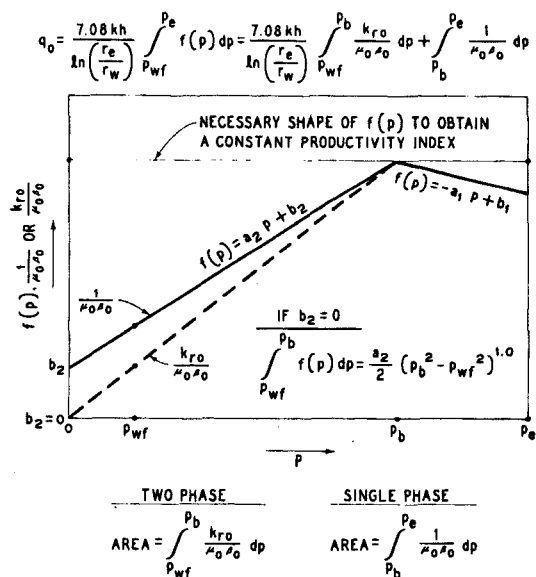


Fig. 2 - Basic pressure function undersaturated oil reservoir.

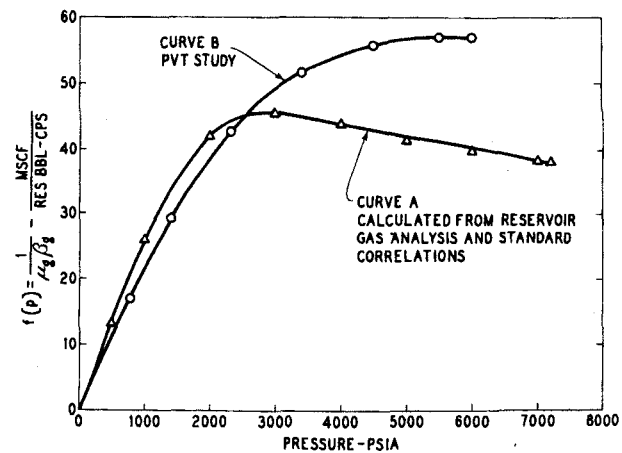


Fig. 3 - Basic pressure function for two high pressure gas reservoirs.

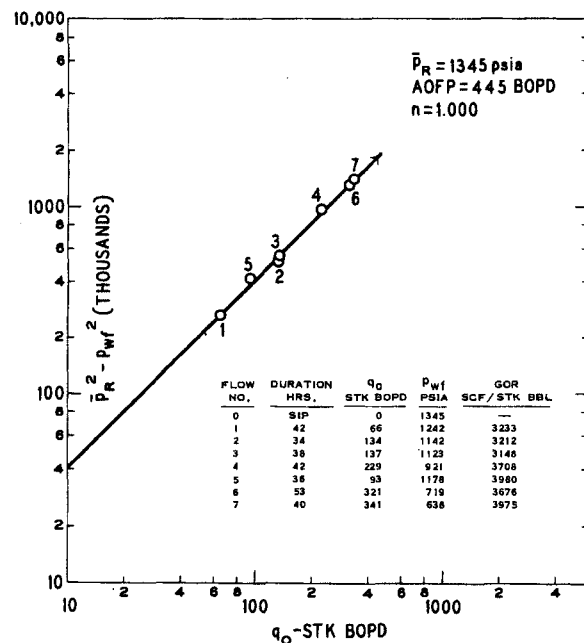


Fig. 5 - Stabilized performance curve, Well 6, Field A.

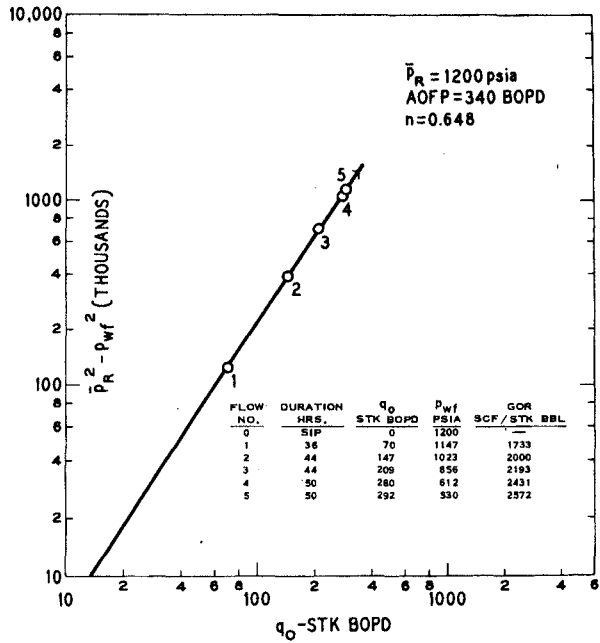


Fig. 6 - Stabilized performance curve of Well 3, Field A.

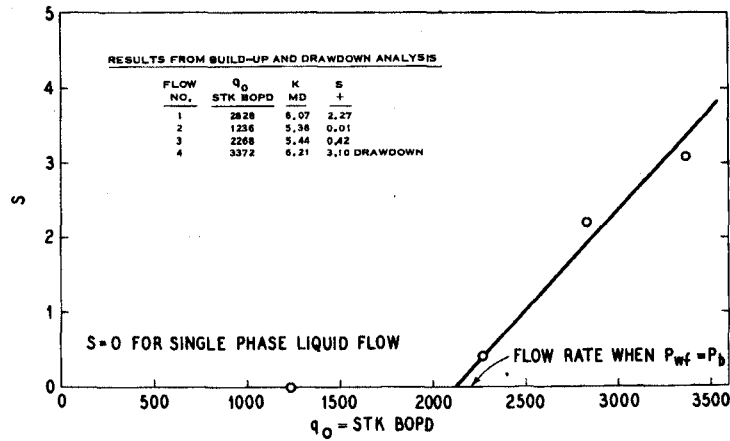


Fig. 7 - Stabilized performance curve of Well 14, Field A.

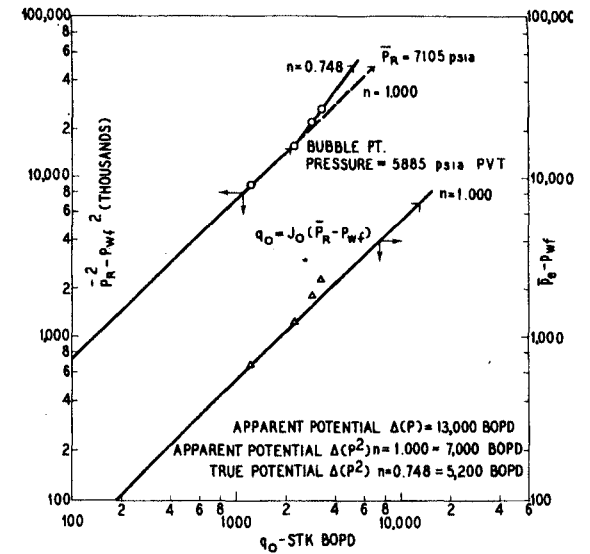


Fig. 8 - Isochronal performance curve of Ekofisk 2/4-2X well, Zone 2, April 14, 1970.

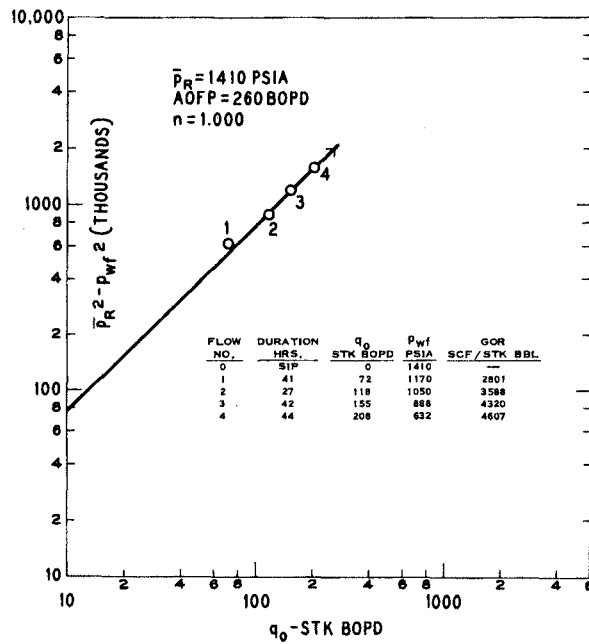


Fig. 9 - Rate-dependent skin effect for flowing pressures less than bubble-point pressure, Ekofisk 2/4-2X well, Zone 2, before acid.

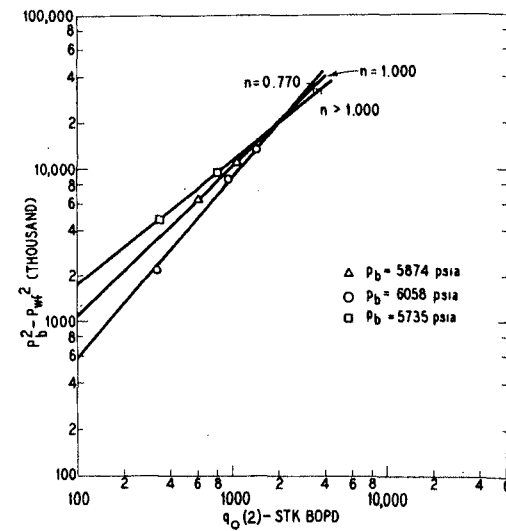


Fig. 10 - Results of trial and error calculations to determine bubble-point pressure of 5,874 psia for Ekofisk 2/4-2X well test on Zone 2.

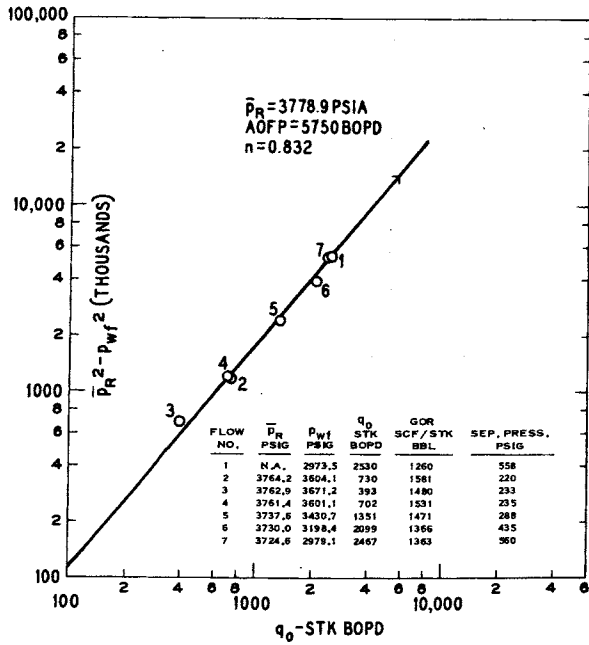


Fig. 11 - Four-hour isochronal performance curve, Well 2-B, Field C, Nov. 30, 1971.

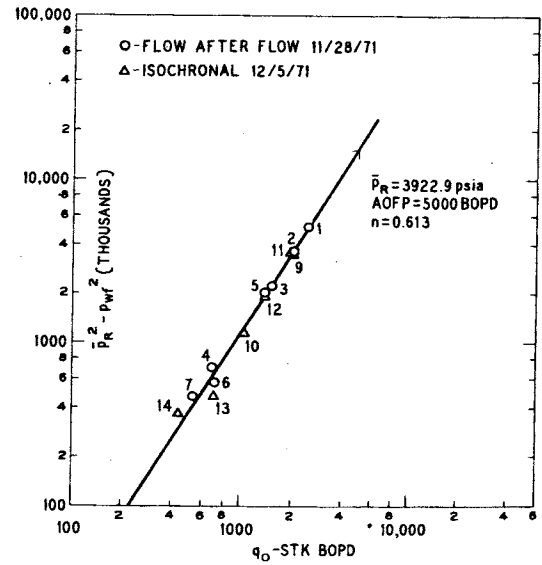


Fig. 12 - Four-hour isochronal and flow afterflow performance curves, Well 3-C, Field C.

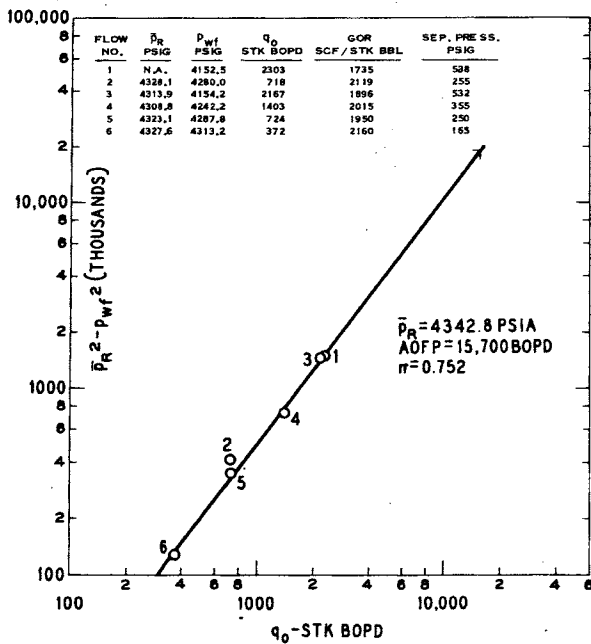


Fig. 13 - Four-hour isochronal performance curve, Well 4-d, Field C, Dec. 10, 1971.

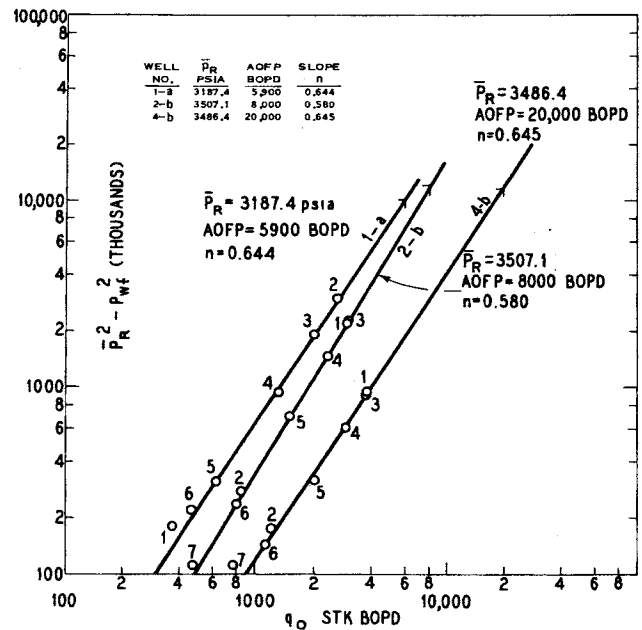


Fig. 14 - Four-hour isochronal performance curves of Wells 1-a, 2-b and 4-b, Field D, demonstrating flow point alignment.

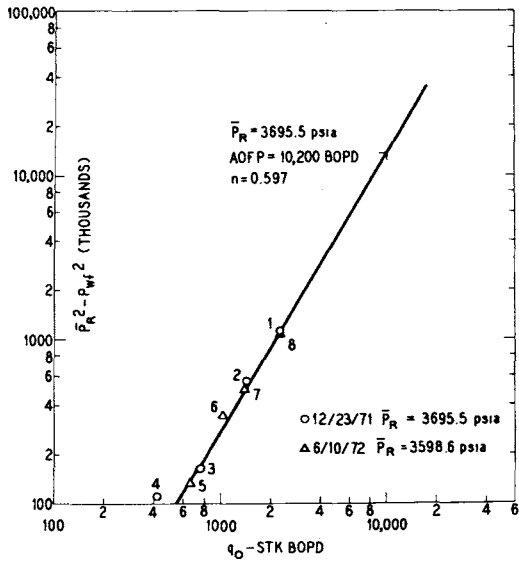


Fig. 15 - Four-hour isochronal performance curves of Well 5-C, Field D.

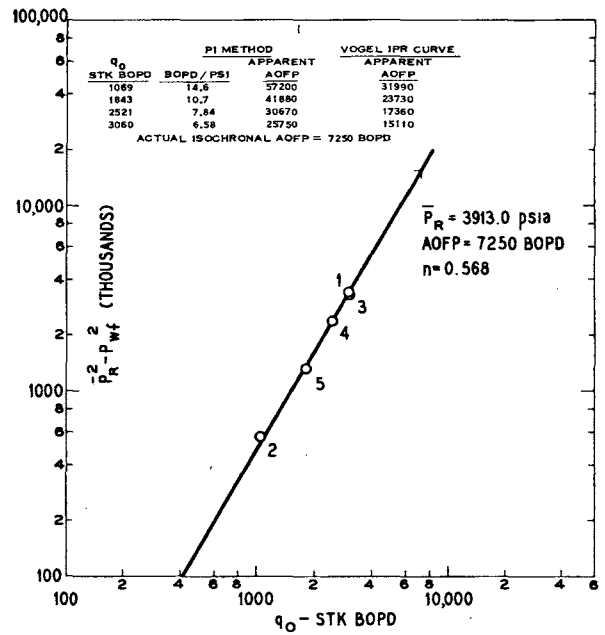


Fig. 16 - Four-hour isochronal performance curve, Well 7-e, Field D, Dec. 14, 1971, with comparisons of calculated AOF's using PI and Vogel methods.

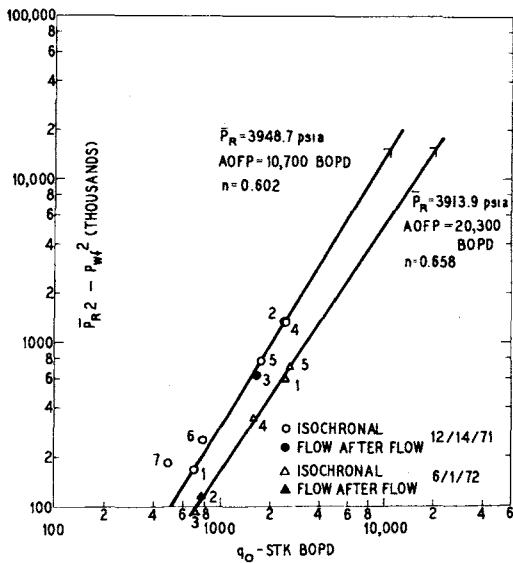


Fig. 17 - Four-hour isochronal performance curves of Well 8-E, Field D, Dec. 14, 1971, with 20 ft of perforations and June 1, 1972, with 60 ft of perforations.

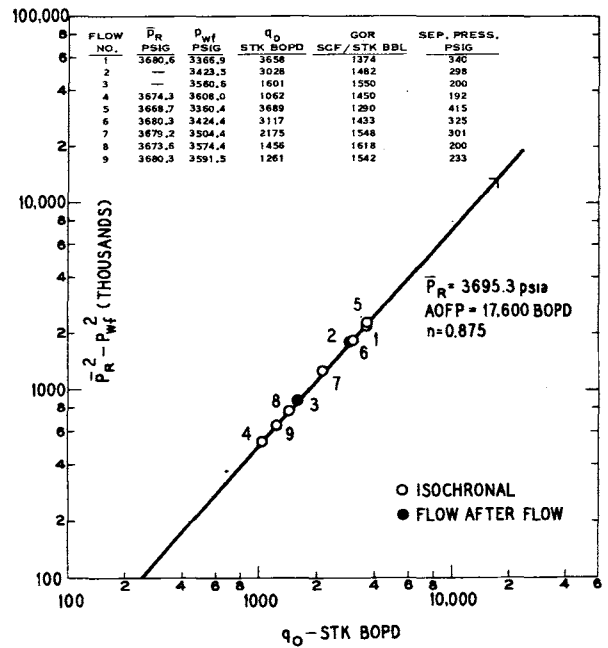


Fig. 18 - Four-hour isochronal performance curve of Well 1-a, Field E, March 16, 1972.

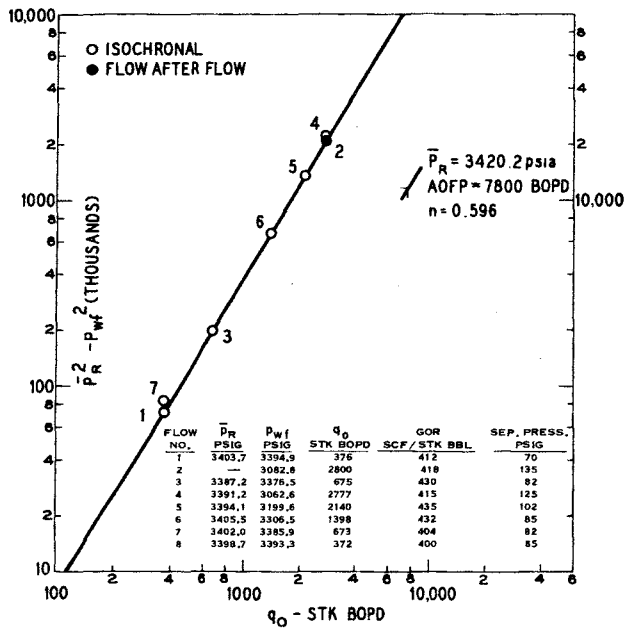


Fig. 19 - Four-hour isochronal performance curve of Well 1-2, Field F, Jan. 2, 1972.

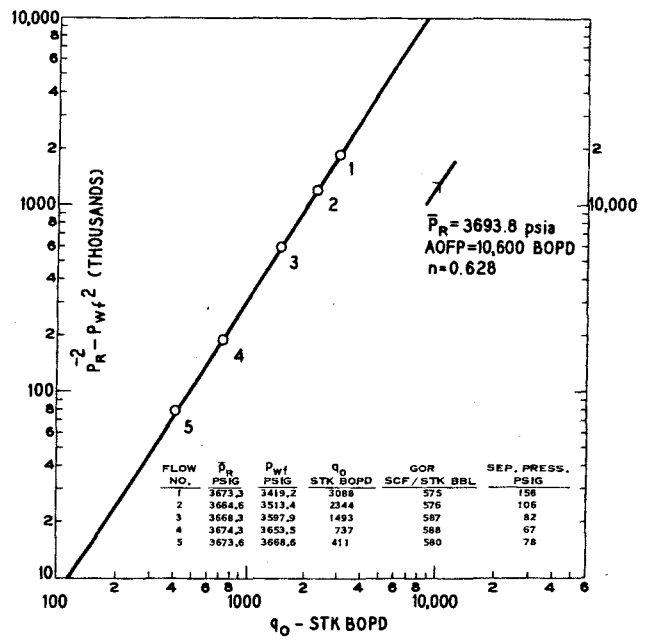


Fig. 20 - Four-hour isochronal performance curve of Well 2-b, Field F, Jan. 7, 1972.

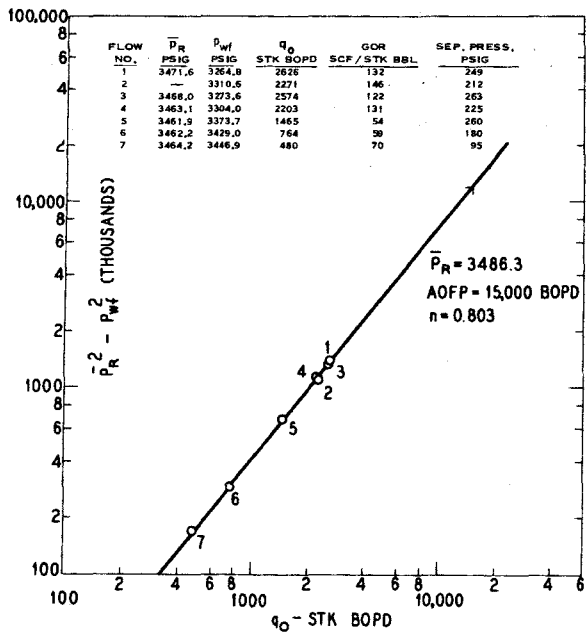


Fig. 21 - Four-hour isochronal performance curve of Well 1-a, Field H, July 24, 1972.

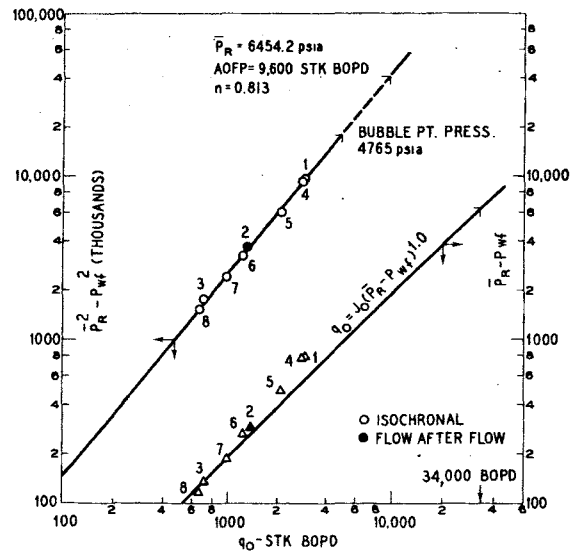


Fig. 22 - Four-hour isochronal performance curve of Well 1-a, Field G, Jan. 18, 1972.

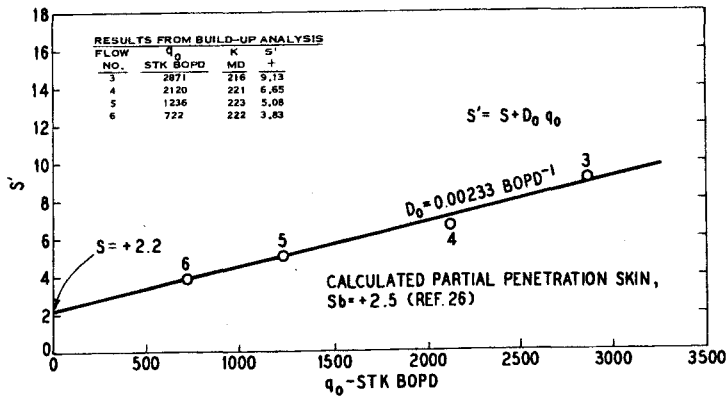


Fig. 23 - Non-Darcy flow effect, single-phase liquid flow, Well 1-a, Field G.

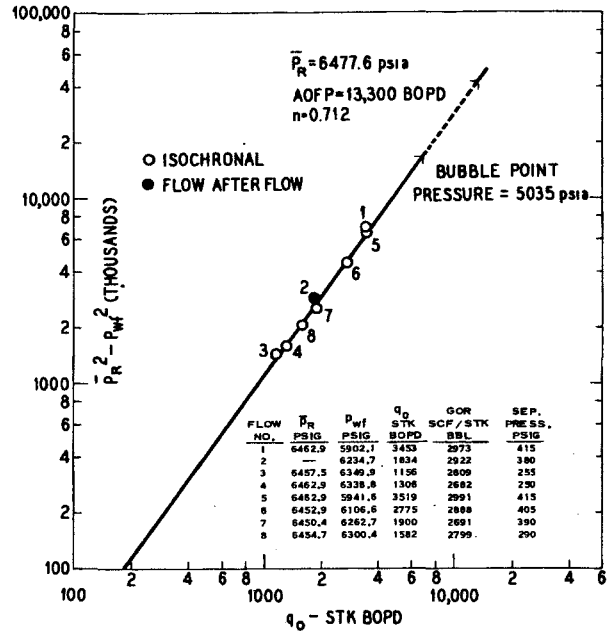


Fig. 24 - Four-hour isochronal performance curve of Well 2-b, Field G, Jan. 8, 1972.

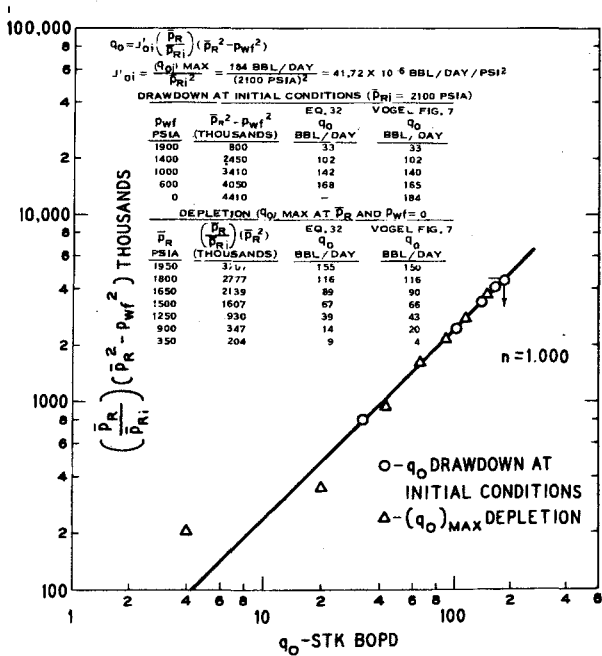


Fig. 25 - Dissolved gas drive drawdown and depletion performance curve (Vogel, Fig. 7).

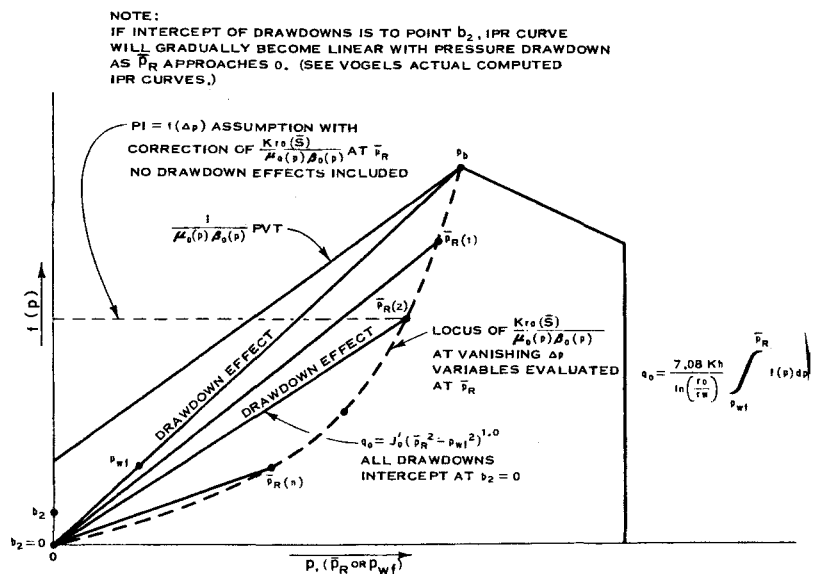


Fig. 26 - Pressure function $f(p)$ illustrating depletion and drawdown.